UNCLASSIFIED

AD NUMBER

ADC055869

CLASSIFICATION CHANGES

TO: unclassified

FROM: restricted

LIMITATION CHANGES

TO:

Approved for public release, distribution unlimited

FROM:

Distribution authorized to DoD only. Other requests shall be referred to Embassy of Australia, Attn: Joan Bliss, Head. Pub. Sec.-Def/Sci, 1601 Mass Ave, Washington, DC 20036.

AUTHORITY

DSTO via ltr dtd 23 Jun 1999; DSTO Library, 23 Jun 99

THIS PAGE IS UNCLASSIFIED

① L

AR-009-403

DSTO-RR-0018

AD-C055 869

Missile Detection by Observation of Differential Motion in an Image Sequence (U)
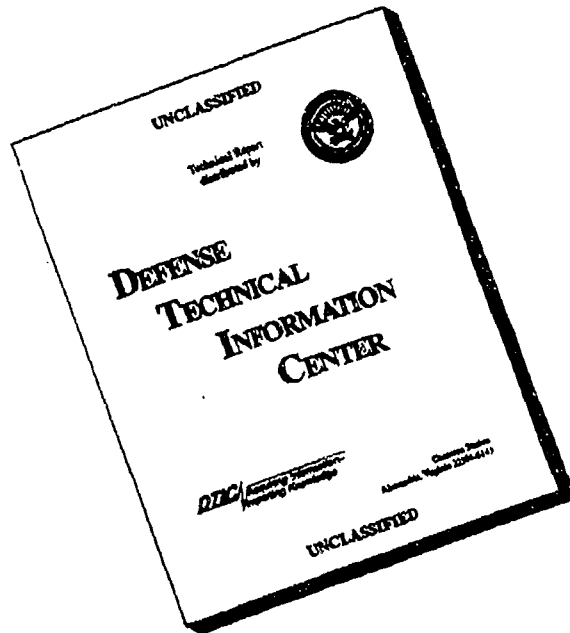
Robert S. Caprari

96-00466 2^3

14

DTIC QUALITY INSPECTED 4

DEPARTMENT OF DEFENCE

DEFENCE SCIENCE AND TECHNOLOGY ORGANISATION

DISCLAIMER NOTICE

THIS DOCUMENT IS BEST
QUALITY AVAILABLE. THE
COPY FURNISHED TO DTIC
CONTAINED A SIGNIFICANT
NUMBER OF PAGES WHICH DO
NOT REPRODUCE LEGIBLY.

Missile Detection by Observation of Differential Motion in an Image Sequence [U]

Robert S. Caprari

Land, Space and Optoelectronics Division
Electronics and Surveillance Research Laboratory

DSTO-RR-0018

ABSTRACT   [U]

This report investigates a technique of passive airborne missile detection by analysing a temporal sequence of images of the ground in the region of the aircraft. Essentially, the technique identifies as potential missiles, objects that move in a different manner to the terrestrial background, as observed in the aircraft reference frame. A kinematical analysis is undertaken to quantify this "differential motion". Brief consideration is given to the observation of this differential motion by image processing techniques. The potential of the technique to localise the missile in space is addressed. The formal kinematics are applied to numerical simulations of guided missile trajectories to quantify the differential motion that occurs, and determine the "warning time" between missile detection and collision. Several operational scenarios are investigated. Simulation results are presented, discussed and appraised, and conclusions drawn about the effectiveness of this technique.

RELEASE LIMITATION

(This page is unclassified)

DOD $ONIY$

Embassy of Australia
Attn: Joan Bliss
Head. Pub. Sec.-Def/Sci.
1601 Massachusetts Ave., NW
Washington, DC 20036

Missile Detection by Observation of Differential Motion in an Image Sequence   [U]

EXECUTIVE SUMMARY

This report addresses the problem of detection of a ground launched missile by an aircraft without relying on radar. Although radar is often a very effective means of missile detection, it is also a beacon inviting and facilitating attack by adversaries. One desires a method of observing a missile based upon light (visible or infrared) being reflected from or emitted by the missile or its exhaust gases. An image of a scene containing such a missile in flight would show the missile as a small, bright spot immersed in a background landscape. Unfortunately, the background has rapid and extreme intensity variations which produce artefacts that are indistinguishable from missiles. Hence, examining individual images, even using the most sophisticated computer algorithms available, will fail to distinguish consistently the real missiles from false alarms.

One strategy to overcome this deficiency in image based missile detection is to examine a sequence of images, and compare later images with earlier ones. Since the aircraft is moving, both the ground and missile images move in time. However, because the missile is typically very much closer to the aircraft, and also because the missile moves relative to the ground, the motions of the missile and ground images are different. The former effect is analogous to the observation that, when walking steadily at night, nearby terrestrial structures (poles, trees, buildings) move into and out of view, while the far away moon seems to follow one around, because its position in the field of view doesn't change.

This report examines the magnitude of the motion difference between the missile and ground, as perceived from the aircraft. It assesses whether the motion is significant enough to enable reliable detection of the missile, and indeed, whether it is possible to estimate the range of the missile from the aircraft just from this motion. Essentially, the conclusion is that it is futile to try to ascertain range by this technique, and while it is probably possible to detect a missile under fairly favourable circumstances, detection performance is not robust enough to be considered reliable.

THIS PAGE IS INTENTIONALLY BLANK

Author

Robert S. Caprari
Land, Space and Optoelectronics Division

Dr Caprari did his undergraduate study at Adelaide University, obtaining the degrees of Bachelor of Engineering (Honours) and Bachelor of Science, the former majoring in electrical and electronic engineering, and the latter majoring in physics. He then joined OED of DSTO as a PO1, and did research in image processing and imaging system characterisation, before joining EWD as a PO2 and doing research in mathematical and acousto-optic applications to radio frequency signal detection and identification. On obtaining DSTO sponsorship as a Cadet RS, he conducted research in experimental and theoretical condensed matter and electron scattering physics at Flinders University, obtaining the degree of Doctor of Philosophy. Subsequently, he joined LSOD in his current position as an RS, undertaking research into theoretical approaches to image analysis and optical approaches to image processing.

THIS PAGE IS INTENTIONALLY BLANK

Contents

THIS PAGE IS INTENTIONALLY BLANK

1   Introduction

A developing threat for aircraft operating in conflict zones is the proliferation of inexpensive, portable and lethal infrared guided surface to air missiles. These weapons are certainly accessible to most conventional armed forces, but of potentially greater concern in a world of disentegrating political axes, is their availability to many rebel armies. There is a growing potential for these weapons to be deployed against aircraft, either in a declared conflict, or in an increasingly common peacekeeping operation.

Having established a requirement for defending aircraft against approaching missiles, one immediately recognises a need for the ability to at least detect approaching missiles, and preferably localise the missile in space. The most effective technique of detecting missiles is by radar. However, radar does have its drawbacks. Radio emissions from the aircraft provide an adversary with advance warning of the approach of the aircraft, which may be of critical assistance to the adversary in mounting an attack on the aircraft. Radar is vulnerable to jamming, thus rendering it inoperable in the most hazardous circumstances. For reasons of cost, weight, size, power or availability, it may not be possible to install a suitable radar system in an aircraft. In future there may even be radar seeking surface to air missiles in the arsenals of technologically advanced adversaries, so further compounding the problems with radar. Consequently, there is a demonstrable need for a passive missile detection scheme; one that produces no electromagnetic emissions.

The subject of this report is the proposal, conceptual development and assessment of one such scheme of passive missile detection. This technique relies on imaging the approaching missile and the ground below it. The 3--5μm infrared band would probably be favoured, because the missile will always be hotter than the background, either because of the hot plume, or skin heating by air friction. Thus the missile infrared signature will usually be conspicuous when it is immersed in any realistic background.

Reliable detection of a missile in individual images is not assured, even when it is very bright, because of the large intensity variation of background clutter. Accordingly, the scheme to be articulated in this report exploits the temporal information available from a time sequence of images, and only seeks prospective missile candidates that have discernible motion relative to the background. This "differential motion" is a consequence of two factors. One is that the missile is actually moving with respect to the background. The other is that the imaging system is moving with respect to both the ground and missile, and the different distances of the ground and missile from the imaging system imply different angular velocities as seen by the imager.

This report addresses the theoretical evaluation of differential motion from the specified motion of aircraft and missile in Sections 2.1 to 2.3. Of course, in practice the motion of the missile, and possibly the aircraft, are not known. Therefore, differential motion must be inferred from the only information that is available, being the image sequence. Image processing operations that assist in this endeavour are nominated in Section 2.4, without elaboration. Although image processing issues are important determinants of the efficacy of the proposed technique, the purpose of this report is primarily to investigate the differential motion that actually occurs, and not necessarily its practical detection.

Section 2.5 addresses the important issue of the possibility of utilising the missile detection technique that is developed here to actually localise the missile in space.

Formulas for the evaluation of differential motion are applied to simulated missile trajectories in Section 3. Aspects of the missile motion simulation are described, as is the application of the differential motion formulas in the context of the simulation. Several simulation results are presented graphically, and discussed in terms of realistic operational scenarios. Section 3 concludes with a qualitative and somewhat subjective appraisal of the simulation results, based upon their implications for useful missile detection performance.

The report ends with some tentative conclusions about the potential of passive missile detection by differential motion estimation from image sequences.

2   Principles of the technique

The only information available to the passive missile detection strategy being investigated is wide field imagery of the ground. This strategy seeks to identify the presen ·· of a missile by discerning its differential motion with respect to the invariant terrestrial background, as observed from the moving reference frame that is the aircraft.

This section contains an exposition of the kinematics of the relative motion of the ground, aircraft and missile. This is followed by analysis that projects this motion in object space onto the image plane. The image plane differential motion that signifies the possible presence of a missile is then identified. Methods of observing the pertinent differential motion in the acquired image sequences are identified in terms of classical image processing operations, to provide a practical context for the preceding analysis. Advice is proffered about the unsuitability of differential motion observation for missile distance determination.

The following reasonable assumptions simplify the analysis. The aircraft velocity has constant direction, and specifically, is horizontal. The aircraft orientation is invariant, and specifically, the body axis of the aircraft is aligned with the velocity vector. The terrain within the field of view is both flat and horizontal. There are no conceptual difficulties associated with the removal of any of these constraints. However, the intricacies introduced into the kinematical analysis by such a generalisation, are not expected to invalidate the insights afforded by the simple analysis that is presented here.

2.1   Kinematical relationships

Define the *Earth* frame O' as a reference frame that is fixed on the Earth, with z' axis pointing vertically downwards. Define the *aircraft* frame O as the reference frame that is parallel to O', but whose origin is always the position of the aircraft. Note that under the prevailing assumptions, the z axis is always the optical axis of the imaging system, and its sense is towards the field of the imaging system. The relationship between these two frames of reference is illustrated in Figure 1.

2
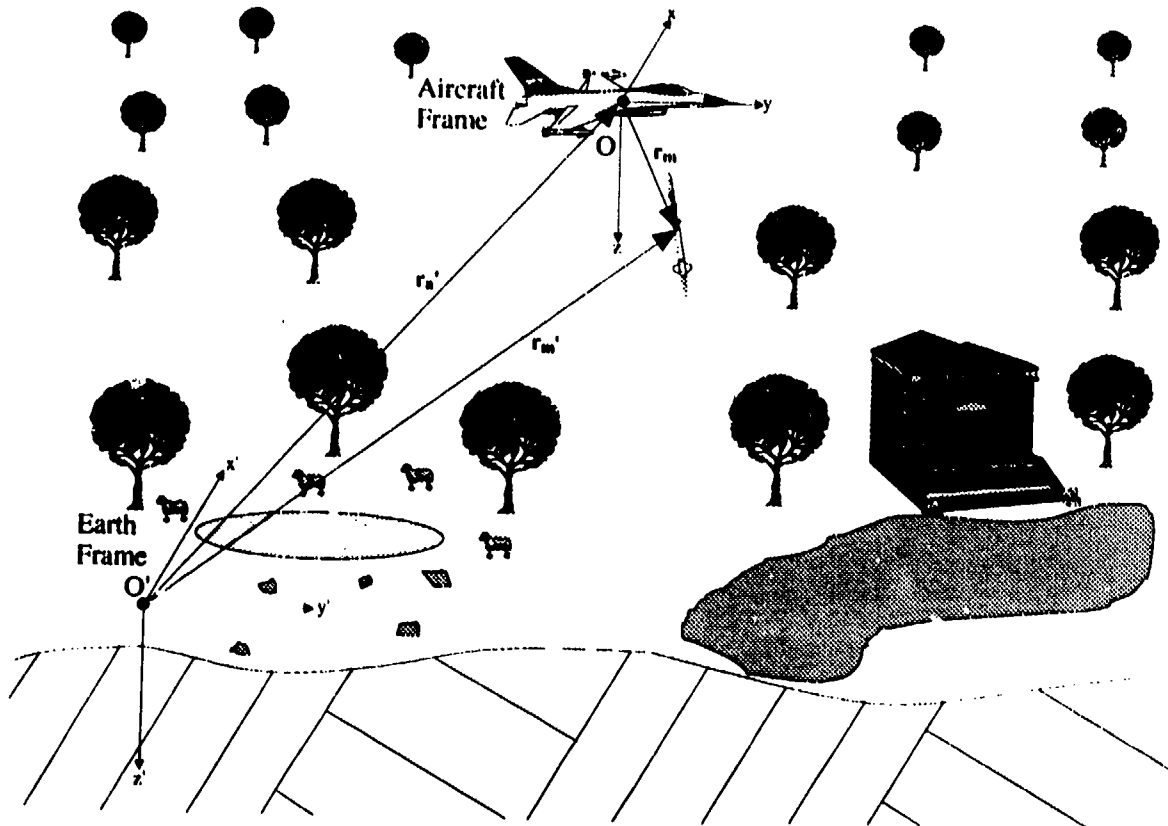
Figure 1: Frames of reference utilised in the differential motion analysis.

The positions of the missile in the Earth and aircraft reference frames, respectively, are (components are specified in cartesian coordinates),

$$\mathbf{r}'_m \equiv (x'_m, y'_m, z'_m) \quad , \quad (\text{frame } O') \quad , \tag{1}$$

$$\mathbf{r}_m \equiv (x_m, y_m, z_m) \quad , \quad (\text{frame } O) \quad . \tag{2}$$

The positions of the aircraft in the Earth and aircraft reference frames, respectively, are

$$\mathbf{r}'_a \equiv (x'_a, y'_a, z'_a) \quad , \quad (\text{frame } O') \quad , \tag{3}$$

$$\mathbf{r}_a \equiv (0, 0, 0) \quad , \quad (\text{frame } O) \quad . \tag{4}$$

As illustrated in Figure 1, these vectors are related by the transformation,

$$\mathbf{r}_m = \mathbf{r}'_m - \mathbf{r}'_a \quad , \tag{5}$$

or in cartesian coordinates,

$$\begin{aligned} x_m &= x'_m - x'_a \quad , \\ y_m &= y'_m - y'_a \quad , \\ z_m &= z'_m - z'_a \quad . \end{aligned} \tag{6}$$

If frame O is specifically defined so that its z axis always coincides with the optical axis, and the orientation of the aircraft were such that an Earth frame O' could not be chosen to be

aligned with O, then (5) and (6) would be modified by the inclusion of a general, possibly time dependent, rotation linear operator, whose matrix representation is an orthonormal 3×3 matrix parametrised by three suitable Euler angles (eg. roll, pitch and yaw).

Equation (6) represents the transformation of the missile and aircraft coordinates in the Earth reference frame, into the position coordinates of the missile relative to the aircraft in the aircraft reference frame. The latter frame is significant, because it is also the imaging system reference frame. Expressing $\mathbf{r}_m$ in spherical polar coordinates (r_m, θ_m, ϕ_m) with respect to frame O, yields

$$
\begin{aligned}
r_m &= (x_m^2 + y_m^2 + z_m^2)^{1/2} , \\
\theta_m &= \arctan (x_m^2 + y_m^2)^{1/2}/z_m , \quad \theta_m \in [0, \pi] , \\
\phi_m &= \arctan y_m/x_m .
\end{aligned}
\tag{7}
$$

Assume stigmatic, but in general distorted, imaging of both the missile and the ground. If the missile image is not resolved, then evidently the missile image may be assigned a unique position. If the missile image is resolved, having significant spatial extent, one may assign the centroid of the image as its unique position. Therefore, one may sensibly represent the missile image position by a unique point in both circumstances. The position of the missile image is completely determined by only the angular coordinates of the missile itself in frame O, that is, θ_m and ϕ_m; exactly how will be elucidated in Section 2.2. Define the background point *conjugate* to the missile, as that location on the ground whose stigmatic image, in the absence of occlusion by the missile, would coincide with the missile image point. The fact that formally the conjugate ground point is never observed in the image due to occlusion by the missile, does not substantively detract from the validity of this analysis, as will be explained in Section 2.4.

An immediate corollary of the discussion of the previous paragraph, is that the angular coordinates in frame O of the missile and its conjugate ground location are identical, that is, denoting the conjugate ground point coordinates by "g" subscripts,

$$
\begin{aligned}
\theta_g &= \theta_m , \\
\phi_g &= \phi_m .
\end{aligned}
\tag{8}
$$

Conjugate missile and ground positions are distinguished by their radial coordinate in frame O, that is,

$$
r_g \neq r_m .
\tag{9}
$$

The ground point that is instantaneously conjugate to the missile is determined from the missile and aircraft positions by the following technique. In the Earth frame of reference, the line of sight from the aircraft to the missile has the parametric equation,

$$
\mathbf{r}'(p) = \mathbf{r}'_m + (\mathbf{r}'_m - \mathbf{r}'_a)p , \quad p \equiv \text{real parameter} .
\tag{10}
$$

Resolving (10) into cartesian coordinates yields,

$$
\begin{aligned}
x'(p) &= x'_m + (x'_m - x'_a)p , \\
y'(p) &= y'_m + (y'_m - y'_a)p , \\
z'(p) &= z'_m + (z'_m - z'_a)p .
\end{aligned}
\tag{11}
$$

4

The flat, horizontal ground coincides with the $x'y'$ plane, so that in frame O' it has the equation,

$$z' = 0 \quad , \quad \text{(ground plane equation)} . \tag{12}$$

Equations (11) and (12) are solved simultaneously to reveal the conjugate ground point $\mathbf{r}'_g$ cartesian coordinates in frame O',

$$
\begin{aligned}
x'_g &= x'_m - \frac{(x'_m - x'_a)}{(z'_m - z'_a)} z'_m \quad , \\
y'_g &= y'_m - \frac{(y'_m - y'_a)}{(z'_m - z'_a)} z'_m \quad , \\
z'_g &= 0 .
\end{aligned}
\tag{13}
$$

In analogy with (6), the conjugate ground point $\mathbf{r}_g$ cartesian coordinates in frame O are,

$$
\begin{aligned}
x_g &= x'_g - x'_a \quad , \\
y_g &= y'_g - y'_a \quad , \\
z_g &= z'_g - z'_a .
\end{aligned}
\tag{14}
$$

Expressing (14) in spherical polar coordinates with respect to frame O, analogously to (7), one obtains,

$$
\begin{aligned}
r_g &= (x_g^2 + y_g^2 + z_g^2)^{1/2} \quad , \\
\theta_g &= \arctan (x_g^2 + y_g^2)^{1/2}/z_g \quad , \quad \theta_g \in [0, \pi] \quad , \\
\phi_g &= \arctan y_g / x_g .
\end{aligned}
\tag{15}
$$

2.2 Imaging transformation

The missile detection strategy being developed here exploits the displacement in the image plane that arises over any finite time interval, due to the differential motion of the images of the missile and its conjugate ground point. Denote the stigmatic imaging of object space point $\mathbf{r}_0(t)$ to image plane point $\mathbf{R}_0(t)$ by the *imaging transformation* $\mathbf{R}$ from a three to two dimensional space,

$$\mathbf{R}_0(t) = \mathbf{R}(\mathbf{r}_0(t)) \quad , \quad \text{(general imaging transformation)} , \tag{16}$$

where parameter t is the time, and all position vectors are with respect to the aircraft reference frame.

The specific form of the imaging transformation $\mathbf{R}$ is dependent upon the distortion of the optical system. The case of perfect imaging (complete absence of distortion) corresponds to $\mathbf{R}$ being a projective transformation [1, Section 4.3]. Perfect imaging is not practicable for the extremely wide field of view optical systems being considered for the present application, which ideally have a 180° field of view. The problem is that as the field of view approaches 180°, the size of the perfect image increases without bound. Consequently, the periphery of the field of view will transgress the finite detection region in the focal plane, and will not be sensed, thereby defeating the purpose of having a wide field optical system.

A much more sensible imaging transformation would have sufficient distortion to map a complete 180° field of view into a finite region of the focal plane. One such imaging transformation is that which actually applies to some types of *fish eye* lenses [2][3, p. 87,88 and 274] and the Zeiss *Pleon* lens [4][5, p. 220]. Define plane polar coordinates (ρ, α) in the image plane, with respect the optical-axis/focal-plane intersection as origin. The spherical polar coordinates in frame O of object space (r, θ, ϕ) are strictly defined with respect to the optical-axis/entrance-pupil intersection as origin. The particular imaging transformation to be considered is, expressed as a polar to polar coordinates transformation,

$$\text{Imaging transformation, } \mathbf{R} : \quad \begin{aligned} \rho &= f\theta \ , \quad \theta \in [0, \pi/2] \ , \\ \alpha &= \phi \ , \end{aligned} \tag{17}$$

where θ is expressed in radians, and f is the effective focal length of the optical system. Note that $\mathbf{R}$ depends only upon the object space angular coordinates θ and ϕ, as anticipated earlier. Imaging transformation (17) exhibits barrel, or positive, distortion. Introducing focal plane cartesian coordinates (X, Y), with respect to the same origin as (ρ, α), one has the final relation,

$$\begin{aligned} X &= \rho \cos \alpha \ , \\ Y &= \rho \sin \alpha \ . \end{aligned} \tag{18}$$

Combining (7), (17) and (18), expresses $\mathbf{R}$ as a cartesian to cartesian coordinates transformation.

Focal length f in (17) is chosen such that the image space, which is a circle in the focal plane, circumscribes the rectangular detector area. If ω (radians) is the field cone half angle (ie. field of view is 2ω), $p_y \times p_x$ is the size of a single detector element and $n_y \times n_x$ is the size of the array of detector elements, then the focal length is chosen as,

$$f = \frac{1}{2\omega}(n_x^2 p_x^2 + n_y^2 p_y^2)^{1/2} \ . \tag{19}$$

2.3   Differential motion

To account for the motion of conjugate ground points, the following notation is introduced: the ground location that is conjugate to the missile at time $t = t_1$ has the position $\mathbf{r}_g(t_1; t_2)$ at time $t = t_2$. Since the surface of the Earth is essentially rigid (any activity that develops in time is assumed to occupy a negligible proportion of the total background), in the Earth frame of reference one has the condition,

$$\mathbf{r}'_g(t_1; t_1) = \mathbf{r}'_g(t_1; t_2) \quad \forall \, t_2 \ . \tag{20}$$

The second time argument in (20) is thus redundant, and one may use the abbreviated notation in the Earth reference frame,

$$\mathbf{r}'_g(t_1) \equiv \mathbf{r}'_g(t_1, t_2) \quad \forall \, t_2 \ . \tag{21}$$

In analogy with (5), one deduces the relation,

$$\mathbf{r}_g(t_1, t_2) = \mathbf{r}'_g(t_1) - \mathbf{r}'_a(t_2) \ . \tag{22}$$

By definition, at an arbitrary time $t = 0$, the missile and its instantaneously conjugate ground point, have coincident images, that is,

$$R(r_m(0)) = R(r_g(0;0)) .$$ (23)

For a moving missile, moving aircraft and stationary background, the instantaneous conjugate ground point diverges with time from that ground location that was conjugate to the missile at $t = 0$; that is, in general at time $t = T$,

$$r_g(T;T) \neq r_g(0;T) .$$ (24)

The differential motion of interest is that between the images of the missile and the ground location that was conjugate to the missile at the instant $t = 0$. Denoting the differential image displacement that occurs as a consequence of this motion during the interval from $t = 0$ to $t = T$ by $\Delta R(T)$, the quantity of interest is,

$$\Delta R(T) \equiv R(r_m(T)) - R(r_g(0;T)) , \quad \text{(differential motion)} .$$ (25)

Expressing (25) as an operation on position vectors in the Earth reference frame, by substituting (5) and (22), one obtains,

$$\Delta R(T) = R(r'_m(T) - r'_a(T)) - R(r'_g(0) - r'_a(T)) .$$ (26)

Note that as a consequence of condition (23), the differential image displacement has the essential property,

$$\Delta R(0) = 0 ,$$ (27)

that characterises any vector that is considered to be a displacement that develops over time.

2.4   Image processing interpretation

The interpretation of differential image displacement (25) in terms of image processing operations is clarified by invoking (23), and expanding (25) to become,

$$\Delta R(T) = [R(r_m(T)) - R(r_m(0))] - [R(r_g(0;T)) - R(r_g(0;0))] .$$ (28)

The quantity $[R(r_m(T)) - R(r_m(0))]$ is measured by identifying the missile image point in each of two images corresponding to the instants $t = 0$ and $t = T$, and evaluating the vector displacement between the two points. This is essentially a manifestation of the classical target identification problem in image processing. If there is more than one missile present, or if there are additional erroneous missile identifications, one must determine the association between individual targets in the initial and final images. Associativity is allocated according to one of the established methods of statistical decision theory.

In principle, the quantity $[R(r_g(0;T)) - R(r_g(0;0))]$ may be measured in an analogous manner, where now it is the conjugate ground point at $t = 0$ that is to be identified

in the two images. In practice this is infeasible, because this point is occluded by the missile in the original image, so that one has no reference with which to identify this point in the final image. However, the fact that the background is extended, and that the variation with position of the background displacement between initial and final images is slow compared with the characteristic length of the background image structure (that is, the image distortion due to optical system motion is slight compared with the intrinsic variation in the background image), offers a feasible method of measuring the displacement $[\mathbf{R}(\mathbf{r}_g(0;T)) - \mathbf{R}(\mathbf{r}_g(0;0))]$.

One may select a region of background surrounding the missile image in the initial image to be a "template". Assuming that the size of the missile image is small compared with the image distortion due to optical system motion, one selects the size of the background region to be much greater than the missile image size. One then optimally matches the final image to this template, by a correlation operation. The resulting displacement of the correlation maximum is interpreted as being the best estimate of the displacement $[\mathbf{R}(\mathbf{r}_g(0;T)) - \mathbf{R}(\mathbf{r}_g(0;0))]$. Although the slight distortion between the two images, and the different positions of the small missile images relative to the background in the two images, will degrade the equivalence between the correlation maximum displacement and the displacement being sought, the stated assumptions ensure that this perturbation is marginal. This procedure is essentially a manifestation of the classical image registration problem in image processing. Since image registration is inherently a nonlocal operation, it is not materially affected by the occlusion of conjugate ground points by the missile, as noted earlier.

In summary, the classical image processing operations of target identification and image registration, possibly supplemented by the decision theoretic operation of associativity, measure the quantities that determine the differential displacement $\Delta\mathbf{R}(T)$ via (28). This establishes another essential property of the definition of $\Delta\mathbf{R}(T)$ (25); the existence of an identifiable procedure for its measurement from the only available information, being sequences of images.

2.5   Suitability of differential motion for missile localisation

Although the detection of a missile is itself a commendable achievement, it is desirable also to determine the missile displacement from the aircraft. Since differential motion observation mandates the use of an imaging sensor, the direction of the missile in the aircraft frame is deducible. The angular coordinates of the missile with respect to the imager optical axis are determined from the missile image plane coordinates by the inverse of the imaging transformation defined by (16). Specifically, one would apply the inverses of (18) and (17) in that order, to convert the missile image coordinates (X_m, Y_m) to the object space angular coordinates (θ_m, ϕ_m).

The only scope for inferring missile range is from the observed differential motion. It is apparent that the differential motion between the missile and conjugate ground point images depends upon the missile trajectory, and indeed, the ground topography. In the

absence of knowledge of these two factors, especially the former, it is not possible to make a credible determination of missile range from differential motion observation.

For instance, there exists a family of stealthy trajectories along which a hypothetical missile could approach the aircraft without the conjugate ground point ever being perturbed. Hence, there would never be any differential motion to observe, and the missile would never be detected. More realistic is the example of a missile whose trajectory in the aircraft frame is always directly towards the aircraft. This is actually a good approximation for the trajectory arising from a *proportional navigation* guided missile approaching an aircraft flying with constant velocity. In such a situation, the position of the missile image is invariant, and any differential motion that is observed is entirely a consequence of the motion of the ground relative to the aircraft. In both of these circumstances, the first rather artificial, but the second quite realistic, it is not even in principle possible to infer the missile range by observing its differential motion, since the missile range does not influence the differential motion.

For a general missile trajectory, the missile range does influence the differential motion in a trajectory dependent manner. If the missile trajectory and ground topography were both known, then there would be a formal solution for the missile range in terms of the differential displacement magnitude. However, in the absence of independent sensing facilities, the missile trajectory in particular is not known, so it is not possible to reliably determine missile range from differential motion observation in realistic circumstances.

In summary, the use of an imaging sensor renders the missile angular coordinates deducible once the missile has been detected by observing differential motion in the image sequence. In contrast, the missile range can not be reliably inferred from differential motion observation in the variable circumstances encountered in practice.

3 Simulation of missile flight and detection

Having established the principles of missile detection by observation of the differential displacement $\Delta \mathbf{R}(T)$, it remains to assess the effectiveness of the technique in scenarios that will be encountered in practice. This is accomplished by simulating the trajectory of a guided missile from launch to engagement of the aircraft, while simultaneously calculating the resulting differential motion.

In this section, the missile trajectory simulation is described superficially, and with the assistance of the exposition of Section 2, a description of the computation of differential motion is presented. Results of particular simulations are presented, discussed and appraised.

3.1 Features of the missile trajectory simulation

Realistic modelling of powered and guided missile flight in the atmosphere is a formidable undertaking. The present investigation was expedited by utilising a missile simulation program furnished by other researchers [6, 7]. This simulation program was modified as

outlined later in this section, and incorporated as an essential element in a differential motion calculation program.

The missile simulation is nominally a 3 degrees-of-freedom approximation of the missile dynamics, in which the three missile position coordinates are the only free kinematical parameters. To account for the thrust direction, the missile orientation is constrained to be tangential to the trajectory. This condition implies two *nonholonomic* constraints (constraints expressed as differential equations; in this case the orientation coordinates determined by the time derivatives of the centroid coordinates [8, Section 1.3]), since orientation is specified by two angles (elevation and azimuth). A third *holonomic* constraint (constraint expressed as an algebraic equation) is that the roll angle of the missile is invariant. These constraints account for the three "missing" degrees of freedom compared with the actual situation. However, to account for the drag on the missile, the inclination of the missile from the trajectory tangent is allowed to be a free pair of parameters (elevation and azimuth). Effectively, the simulation is a "3 and a bit" degrees-of-freedom approximation of the missile trajectory.

Ironically, the presence of nonholonomic constraints in the simplified model of missile dynamics implies that, even in principle, the equations of motion probably do not have a formal solution. In the absence of formal analytic solutions, the present simulation numerically solves the equations of motion by finite difference methods.

The approximate nature of the missile model inevitably causes a significant discrepancy between the simulated trajectory and the actual trajectory. The severity of this discrepancy has not been quantified, but the author believes that this simulation is at least qualitatively correct, and that the quantitative errors are not so extravagant as to render the simulation unrepresentative of realistic missile motion.

The missile characteristics utilised in the present simulations have been selectively modified from those existing in the original simulation. Variation of mass and thrust with time, external dimensions for evaluation of drag, fuel load for range determination and the guidance law (proportional navigation in this case), are all representative of an actual missile. However, unlike any real missile, in these simulations there is no maximum limit on the angular velocities or angular accelerations of either the missile body or the seeker head; effectively the missile and seeker have zero rotational inertia. Furthermore, there is also no maximum limit on the angular displacement of the seeker axis from the missile axis.

Although the original missile simulation algorithm did impose bounds on the achievable missile dynamics, these bounds were deliberately removed from the missile model used for the present simulations to enable a more extensive test of the detection algorithm. It transpires that with the manoeuvrability bounds set at realistic values, there is typically a large region on the ground within which a launched missile fails to engage the aircraft, according to the original missile simulation. By removing the selected constraints, the engagement launch envelope has its "voids" significantly, but not entirely, filled in. Since one is most interested in assessing the performance of the missile detection algorithm, and not the missile's ability to engage its target, it is beneficial to manipulate the missile characteristics to maximise the opportunities of testing the detection algorithm (such a test requires the missile to intercept the aircraft).

Removal of the missile dynamics bounds almost certainly increases the inaccuracy of the missile trajectory simulation beyond that which already afflicted the original simulation. No attempt was made to gauge the severity of degradation of accuracy. The author is of the opinion that this further compromise in accuracy does not materially affect the qualitative assessment of the results of these investigations. However, the existence of this further source of inaccuracy does reinforce the need for caution in the interpretation of the results. A prudent and justifiable policy to adopt, would seem to be only to draw qualitative conclusions from one's assessment of the results.

3.2 Computation of differential motion

Having solved the missile motion, knowing the uniform aircraft motion and knowing that the ground is rigid, sufficient information is now available to compute the differential motion $\Delta \mathbf{R}(T)$ from the kinematical considerations enunciated in Section 2.

The missile trajectory computation furnishes cartesian coordinates of the missile position vector $\mathbf{r}'_m$ in the Earth frame. The cartesian coordinates of the aircraft position vector $\mathbf{r}'_a$ in the Earth frame are defined by the motion of the aircraft. Having chosen a suitable time interval T for the displacements to develop, the differential motion at arbitrary time $t = 0$ is evaluated by the direct application of (26). As explained in Section 2.2, imaging transformation $\mathbf{R}$ is expressed as a cartesian (R^3) to cartesian (R^2) coordinates operation by combining (7), (17) and (18).

3.3 Method of presentation of simulation results

Aspects of the computation of the differential motion corresponding to a single missile launch position have been addressed in Sections 3.1 and 3.2. To obtain full coverage of the ground, these simulations are repeated on a relatively fine grid (40 to 100 metres spacing) of launch sites on the ground. The grid of launch sites extends beyond the range of the missile to encompass the complete threat region.

The results of this substantial simulation are best interpreted if one evaluates a single critical parameter as a scalar field, with the argument being the launch position. Undoubtedly, the most critical parameter is the *warning time*, defined as the time that elapses between the differential motion algorithm first deciding that a missile is present, and the missile actually engaging the aircraft. Results of the current simulations are displayed as quantised intensity plots of the warning time scalar field (often referenced as warning time "maps" in this document).

All simulations correspond to a constant velocity aircraft. The simulation program actually does accomodate climbing (positive elevation from horizontal) or descending (negative elevation) aircraft, despite the kinematics established in Section 2.1 assuming horizontal flight. Axes of the parallel reference frames O and O' are oriented with respect to the aircraft as illustrated in Figure 1, that is; x, x'—from right to left; y, y'—from rear to front; z, z'—downwards along the optical axis. The aircraft velocity is along the positive

y' direction. A non-zero elevation is achieved by rotating the aircraft body and its velocity about the x axis, in a clockwise sense through the prescribed elevation angle.

Regardless of the aircraft elevation, there is reflection symmetry of the kinematics in the $y'z'$ plane. Accordingly, the warning time field is only computed and displayed for launch positions with $x' \geq 0$; the field for $x' < 0$ is implied by reflection in the y' axis. In all of the displayed maps, the aircraft position at the instant of missile launch is such that $x' = 0$, $y' = 0$ and $z' < 0$. The position coordinates of the maps are the x' and y' coordinates of the missile launch site, and the launch position specification is completed by setting $z' = -1$ metres.

The algorithm decides that it has detected a missile according to the following simplistic, but reasonable, heuristic decision process. The differential displacement vector $\Delta\mathbf{R}(T)$ is expressed in units of horizontal and vertical detector element dimensions, and its Euclidean norm is compared with a prescribed threshold. If this threshold is exceeded for a prescribed number of consecutive images in the sequence, the algorithm decides that it has detected a missile. The time at which the missile is detected is noted, but the missile trajectory computation continues until engagement of the aircraft, this time also being noted. The warning time is defined as the time that elapses between the missile being detected and the missile engaging the aircraft.

The displayed maps indicate several intervals of warning time by different intensities. Black shading generally corresponds to zero warning time, that is, the algorithm fails to detect the missile at any time before engagement. The one possible exception to this rule is the region in the vicinity of the origin of the $x'y'$ plane. The missile trajectory simulation program is unstable (ie. the computed motion diverges rapidly from a realistic trajectory) in this region, and one adopts the conservative approach of assigning a zero warning time within this region. The extent of this region is chosen to be a circle that subtends an angle of $10°$ from the vertical at the aircraft initial position. White shading always indicates failure of the missile to engage the aircraft, regardless of whether the missile was detected before the trajectory simulation was terminated. Since all maps extend beyond the range of the missile, they all have white regions on their periphery. Regions of lighter shading on individual maps signify longer warning time intervals. Except for black and white regions, there is in general no warning time equivalence between regions of the same shading in different maps. Accordingly, one must exercise caution when comparing different maps; in particular, one should not necessarily attach the same significance to regions of identical shading in different maps.

The elapsed time interval T for the development of displacements from the differential motion, is always chosen to be an integral multiple of the time interval separating consecutive images in the sequence of images. Several aircraft dispositions are considered in the simulations. For each disposition, all imaging and algorithm parameters are invariant, except for T. Warning time maps are computed for three different values of T for every aircraft disposition. This facilitates assessment of the crucial influence that T exerts on the attainable warning times. There is comparative flexibilty in the choice of T, since it is essentially a software parameter, and is not influenced by the optical system apparatus.

12

3.4 Discussion of warning time maps

Computed warning time maps corresponding to seven realistic operational scenarios are displayed in Figures 2 to 8 on pages 18 to 45. Features of the warning time maps are identified and discussed in this section, without consideration at this stage of the implications of the simulation results. The latter undertaking is reported in Section 3.5.

The warning time maps of Figure 2 are representative of a high speed aircraft in transit. Only the time interval T within which the differential displacement develops differs among the three maps. A significant void in the warning time map, within which the missile fails to engage the aircraft, is evident as the irregularly shaped white region intruding into an otherwise convex shaded region of successful engagement. Such voids are present to varying degrees in other warning time maps. The extent to which the warning time maps as a whole, and the voids in particular, accurately reflect real missile performance, is dependent upon the quality of the missile trajectory calculation. As indicated in Section 3.1, this computation is not, nor is it designed 'o be, particularly accurate. Comparing the three maps demonstrates that within much of the region of successful engagement, the warning time increases noticeably with increasing integration time T, as expected, and consistent with most other scenarios investigated.

The warning time maps of Figure 3 are representative of very fast flight at moderate altitude. In this situation, the void in the warning time map particularly severely curtails the engagement envelope. To some extent this may be due to lack of anticipation in the choice of initial missile direction; the missile is always launched directly towards the aircraft, regardless of the aircraft speed. Once again, detection of the missile improves dramatically with integration time T.

The warning time maps of Figure 4 are indicative of a transport aeroplane having just taken-off (note the positive elevation). The upward elevation of the aircraft, together with its low altitude, are such that a missile launched from far behind the aircraft will approach the aircraft nearly horizontally, so the missile will be beyond the imaging system field of view. Consequently, such a missile will never be detected, regardless of the integration time T. This inference is confirmed by the three warning time maps, all of which exhibit vanishing warning time for launches that are far enough behind the aircraft.

The warning time maps of Figure 5 are illustrative of an aircraft on a jungle reconnaissance mission. Within almost all of the engagement launch envelope there is no warning. Further simulation demonstrated that if the field of view is increased to 180°, then the region of no warning is reduced by a moderate amount, but still dominates the warning time map. These warning time maps are anomalous in the sense that the warning time does not increase monotonically with integration time (map (c) has the longest integration time, but the shortest warning time). This result cautions one against assuming that missile detection performance necessarily increases with integration time with no limit, even for very long integration times. It doesn't!

The warning time maps of Figure 6 represent very low altitude, high speed flight. For these maps the optical system field of view has had to be increased to a full hemisphere to obtain any detection at all. The fact that a slight increase in field of view from 160° to 180° has transformed the missile detection performance from complete failure to quite

satisfactory, attests to the critical influence of the optical system field of view on missile detection by very low altitude aircraft.

The warning time maps of Figure 7 are indicative of a transport aircraft during long distance transit. The performance of the differential motion missile detection technique shows substantial improvement with integration time.

The warning time maps of Figure 8 are illustrative of a helicopter cruising horizontally. This simulation considers the helicopter to be oriented horizontally, instead of having its nose inclined downwards to achieve forward motion, as for actual helicopter flight. These warning time maps are all distinguished by the complete absence of voids in the engagement launch envelope. The warning time that is achieved by the differential motion observation increases with integration time.

3.5 Appraisal of warning time maps

One seeks to assess the performance of the differential motion missile detection technique on the basis of the warning time maps of Figures 2 to 8. Apart from the rather exceptional scenario represented by Figure 5, where the missile was usually at the periphery of the field of view and the integration times were relatively long, the warning time increases with integration time. Therefore, each scenario will be assessed on the basis of its longest T warning time map, being map (c) in each figure. One will arbitrarily, but realistically, presume that warning times of less than 2 seconds are totally inadequate, those of 2–4 seconds are marginally useful, and those above 4 seconds are satisfactory.

Figure 2(c) exhibits a reasonable area of successful detection, but there remains a significant region of unsuccessful detection in the forward direction. The performance of the missile detection algorithm would probably improve demonstrably with an even longer integration time. However, in the absence of confirmation of this hypothesis, one concludes that for this scenario, missile detection fails for an unacceptably large region.

Figure 3(c) indicates quite successful missile detection within most of the engagement launch enveope. The only exception is a small region towards the exteremity of the engagement envelope in the forward direction. Increasing the integration time could render the missile detection successful essentially everywhere within the launch envelope for this scenario.

Figure 4(c) is characterised by the majority of the region within the launch envelope corresponding to unsuccessful missile detection. Furthermore, for much of the region behind the aircraft, the failure to detect the missile is probably due to the missile flying above the extremity of the field of view. Increasing the field of view to a full hemisphere would probably improve the missile detection performance in the backward direction significantly. Further enhancement of the missile detection capability would accrue from increasing the integration time. However, on the basis of existing evidence, missile detection by differential motion is unsatisfactory for this scenario.

All three warning time maps of Figure 5 emphatically confirm that missile detection by differential motion is most unsatisfactory in this scenario. These computations suggest

that there are no advantages to be gained by increasing the integration time even further. The limiting factor in the performance of the missile detection algorithm over much of the region is the field of view. Expanding the field of view to 180° yields a moderate increase in warning time over much of the region, however, the overall performance of the missile detection strategy remains inadequate for this scenario.

Figure 6(c) shows satisfactory missile detection performance within most of the engagement launch envelope, an outcome that is only enabled by using a 180° field of view. The regions for which missile detection is inadequate would probably be reduced in size by an increase in integration time. Hence, missile detection by differential motion is quite successful for this scenario.

Figure 7(c) exhibits successful missile detection within much of the engagement envelope, although there remains an intolerably large region in the forward direction within which missile detection is unsuccessful. Increasing integration time should have a moderately beneficial impact on missile detection performance, but on the basis of only the presented evidence, the performance is inadequate.

Figure 8(c) exhibits approximately equal areas within the engagement envelope corresponding to each of the inadequate, marginal and satisfactory missile detection categories. One could expect a modest increase in warning times with an increasing integration time, but even with this enhancement, the overall missile detection performance would still be inadequate for this scenario.

4 Conclusion

The differential motion missile detection simulations that have been presented in this document, while not exhaustive, have elucidated some important factors that influence the performance of missile detection. Maximising the field of view has considerable benefits, which are especially dramatic for low flying aircraft. Increasing the integration time within which the differential displacement is allowed to develop is the other factor that dramatically improves performance, under almost all circumstances.

Nevertheless, on the basis of the present calculations, one would conclude that differential motion observation does not provide one with a reliable missile detection strategy over a diversity of scenarios. The number of simulations that have been conducted is insufficient to convey an indication of any pattern in the success of the algorithm in different scenarios, if indeed such a pattern even exists. Given the nature of the differential motion technique, its missile detection performance depends critically on the missile trajectory. Therefore, it would probably be futile to seek such a hypothetical pattern, since it would almost certainly vary with different missile trajectories, thus not being of general validity.

There certainly is scope for more detailed investigation of the effect of various factors on missile detection by differential motion observation. Given the reservations expressed about the validity of the missile trajectory computation employed in the present investigations, perserverance with the current simulations is not recommended for discerning

subtle patterns in the outcome, which may be destroyed by, or even arise from, simulation inaccuracy. However, the author is of the opinion that the qualitative assessment of the technique stated here will not be overturned by further accurate simulation: that differential motion observation has the potential to detect approaching missiles only under specific circumstances that are too restrictive for it to be considered a candidate for the primary missile detection strategy.

Regardless of whether differential motion observation is deemed a satisfactory means of detecting missiles, it has been argued in Section 2.5 that it is certainly not a reliable method of determining missile range. This detracts further from the attractiveness of differential motion observation as the primary missile detection strategy. It seems that at best, observation of differential motion should only be used to augment another generally superior missile detection strategy, if indeed there is a need for such a supportive role.

A further comment on the scope of these investigations may be appropriate. The advice proffered above relates only to the possibility of ranging or detection of missiles by observation of differential motion. In no way should it be construed as having relevance to any other passive ranging and detection techniques, other infrared techniques, or other image processing techniques that seek to achieve the same capability.

Acknowledgements

16

References

1. M. Born and E. Wolf, *Principles of Optics*, 6th ed., Pergamon Press, Oxford (1980).

2. K. Miyamoto, "Fish eye lens", J. Opt. Soc. Am. **54**, 1060-1061 (1964)

3. R. Kingslake, *Optical System Design*, Academic Press, New York (1983).

4. I. C. Gardner and F. E. Washer, "Lenses of extremely wide angle for airplane mapping", J. Res. Natl. Bur. Svd. **40**, 93–103 (1948); also J. Opt. Soc. Am. **38**, 421–431 (1948).

5. R. Kingslake, "Illumination in optical images", Chapter 5 in *Applied Optics and Optical Engineering*, Volume II, R. Kingslake (ed.), Academic Press, New York (1965).

6. R. C. Lane, "A flexible model for obtaining the coverage performance of guided missiles", WRE Technical Note 676 WR&D (1972).

7. R. Anderson, private communication (1994).

8. H. Coldstein, *Classical Mechanics*, 2nd ed., Addison-Wesley, Reading MA (1980).

Figure 2

(next three pages)
List of common parameter values.

Number of pixels in the x direction = 512
Number of pixels in the y direction = 512
Pixel period in the x direction = 50.0 μm
Pixel period in the y direction = 50.0 μm
Field of view cone half angle = 80.0°
Frame rate = 25.0 s^{-1}
Detection threshold displacement = 2.00 pixels
Required consecutive missile detections = 4
Initial height of aircraft = 983.0 m
Upwards elevation = 0.0°
Aircraft ground speed = 1075.0 km/h

Warning times (seconds) corresponding to intensity levels:
- 0 (no warning; black region)
- 0-3
- 3-6
- 6-9
- 9-12
- ∞ (no engagement; white region)

MISSILE DETECTION MAP
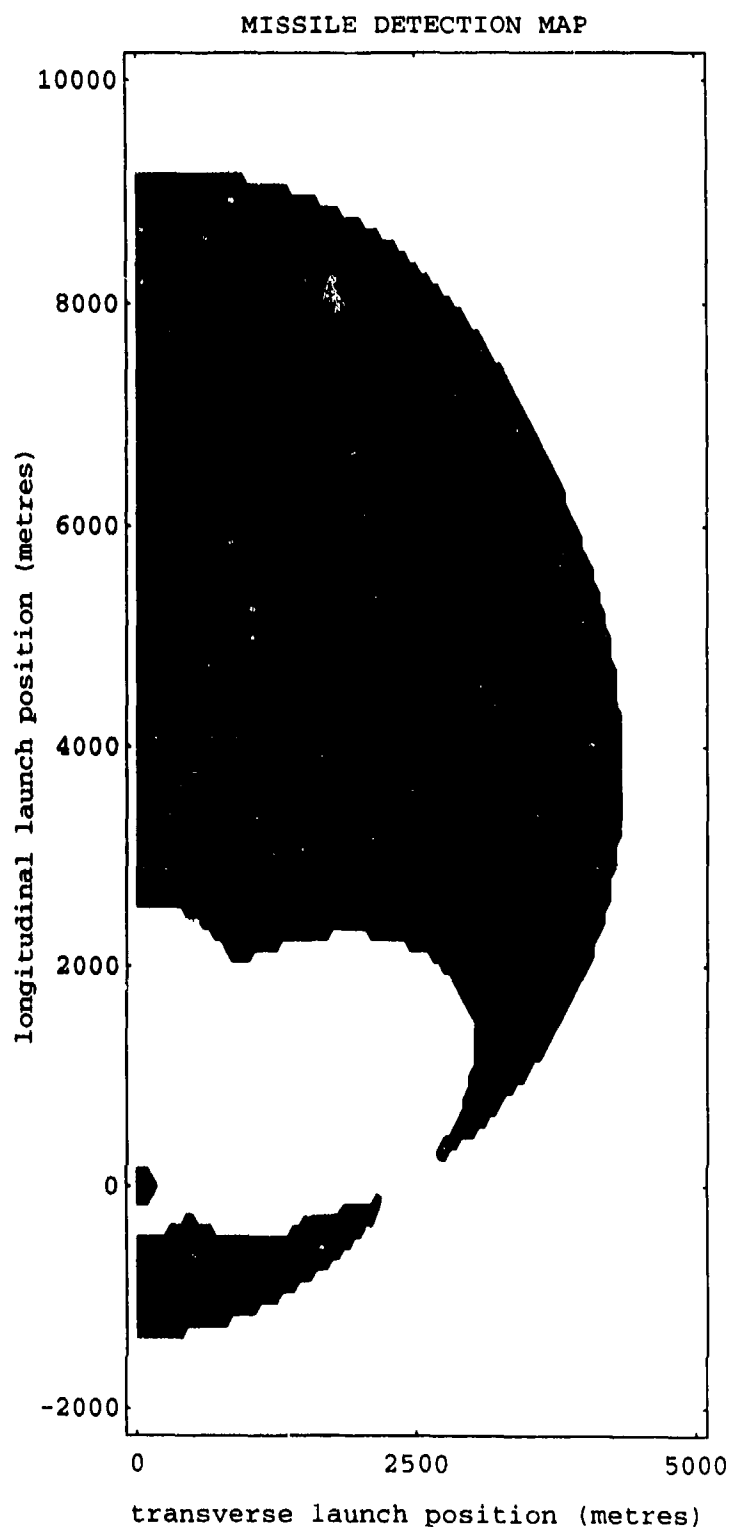
Figure 2: (a) Time interval for differential displacement to develop = 2 frames.

19

MISSILE DETECTION MAP
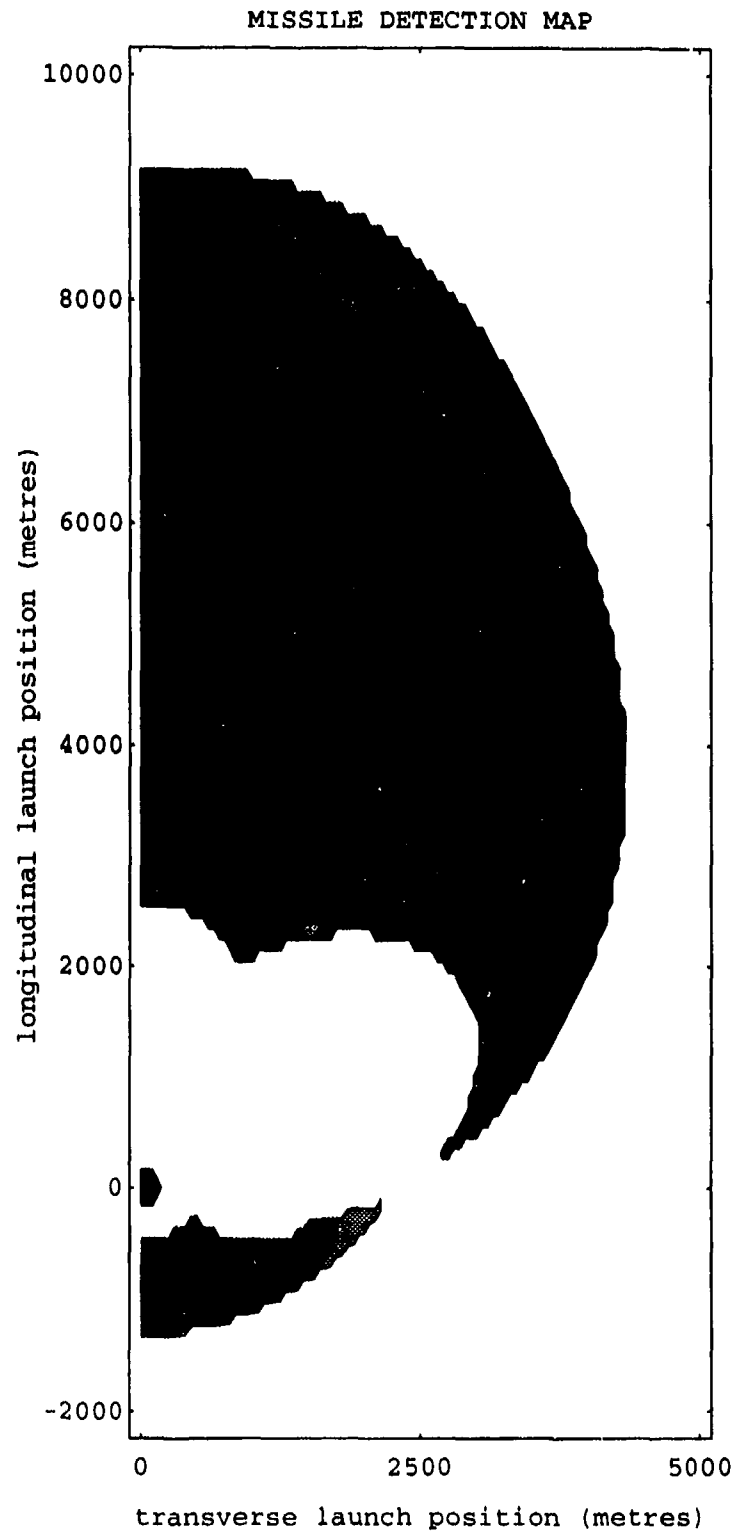
Figure 2: (b) Time interval for differential displacement to develop = 6 frames.

map 03
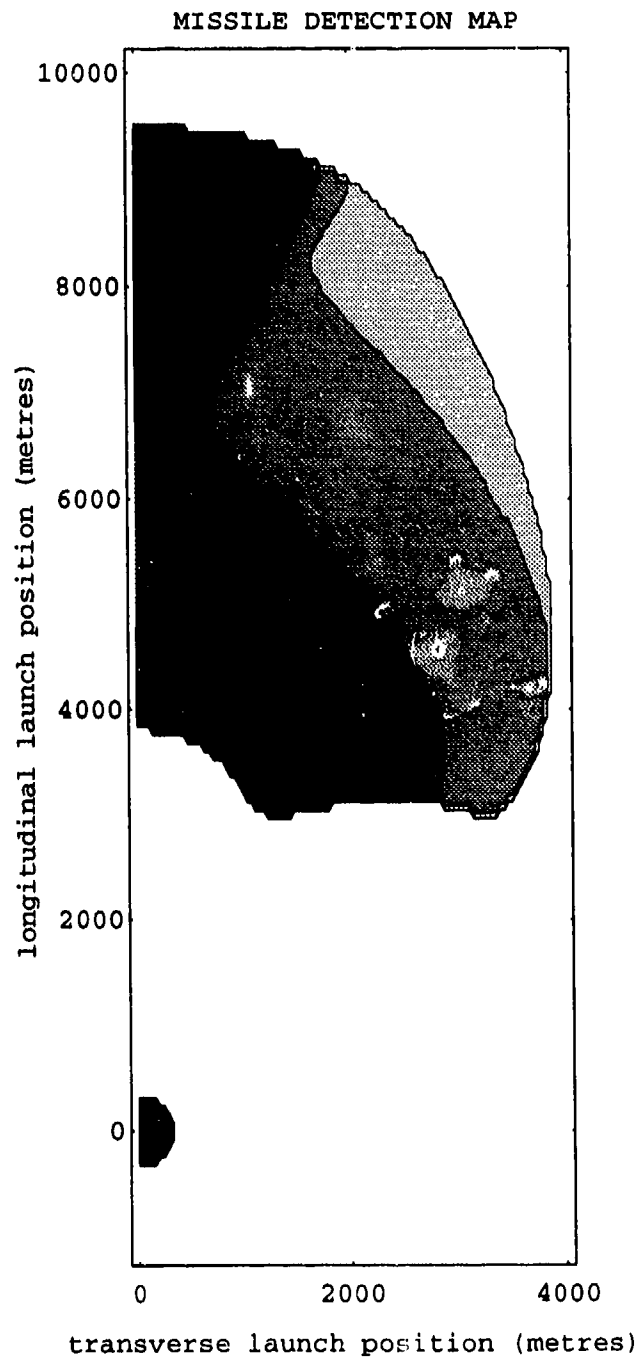DSTO-RR-0018

MISSILE DETECTION MAP
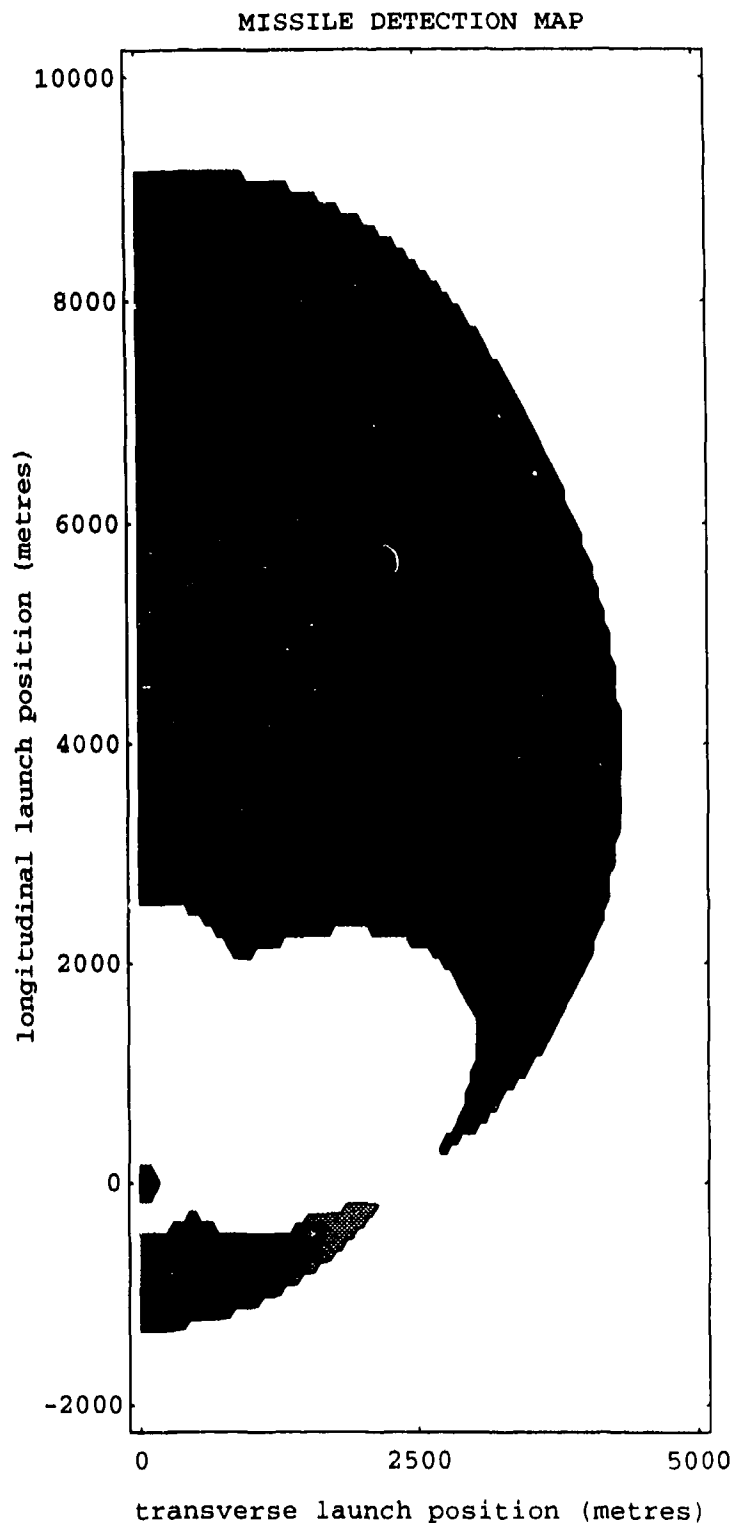
Figure 2: (c) Time interval for differential displacement to develop = 10 frames.

21

Figure 3
(next three pages)
List of common parameter values.

Number of pixels in the x direction = 512
Number of pixels in the y direction = 512
Pixel period in the x direction = 50.0 μm
Pixel period in the y direction = 50.0 μm
Field of view cone half angle = 80.0°
Frame rate = 25.0 s^{-1}
Detection threshold displacement = 2.00 pixels
Required consecutive missile detections = 4
Initial height of aircraft = 1764.0 m
Upwards elevation = 0.0°
Aircraft ground speed = 1356.0 km/h

Warning times (seconds) corresponding to intensity levels:
- 0 (no warning; black region)
- 0–2
- 2–4
- 4–6
- 6–8
- 8–10
- ∞ (no engagement; white region)

MISSILE DETECTION MAP
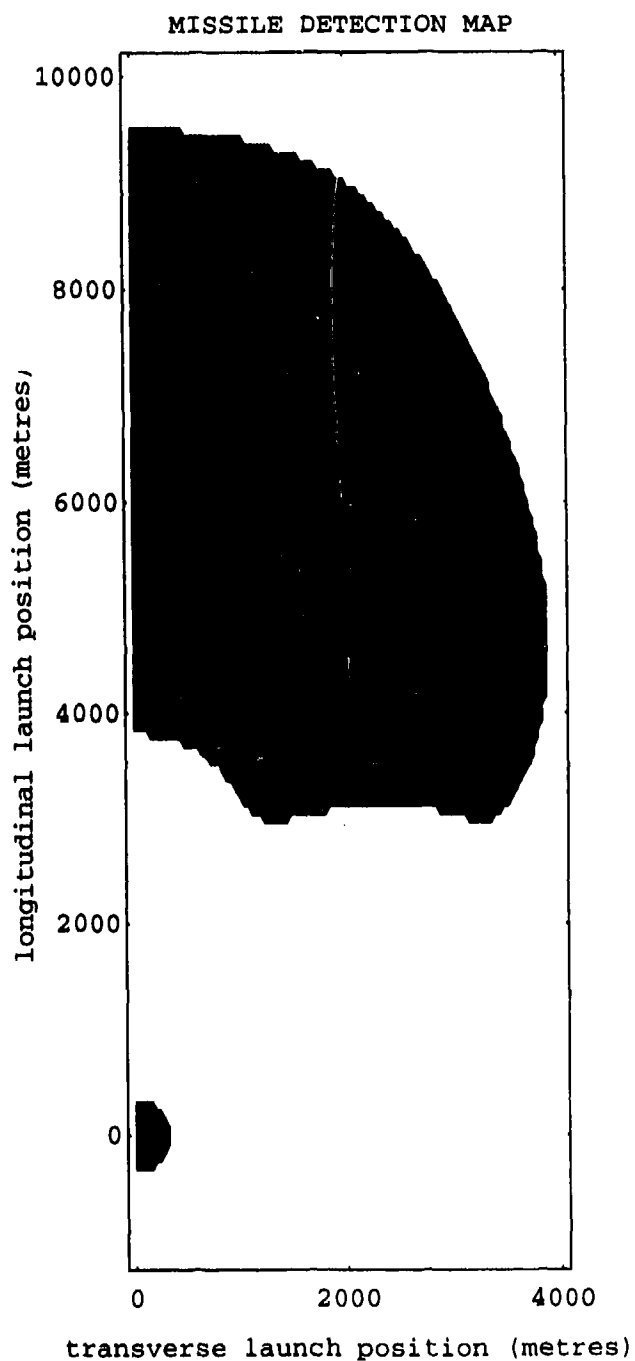
Figure 3: (a) Time interval for differential displacement to develop = 3 frames.

23

MISSILE DETECTION MAP
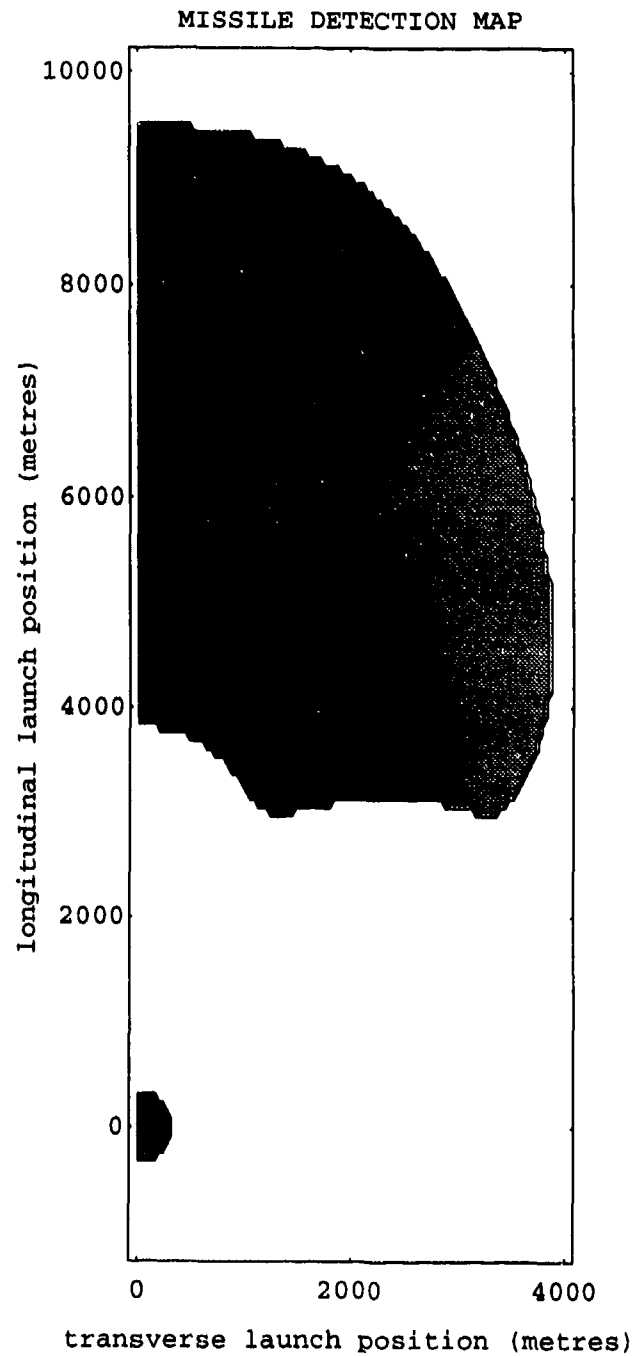
Figure 3: (b) Time interval for differential displacement to develop = 8 frames.
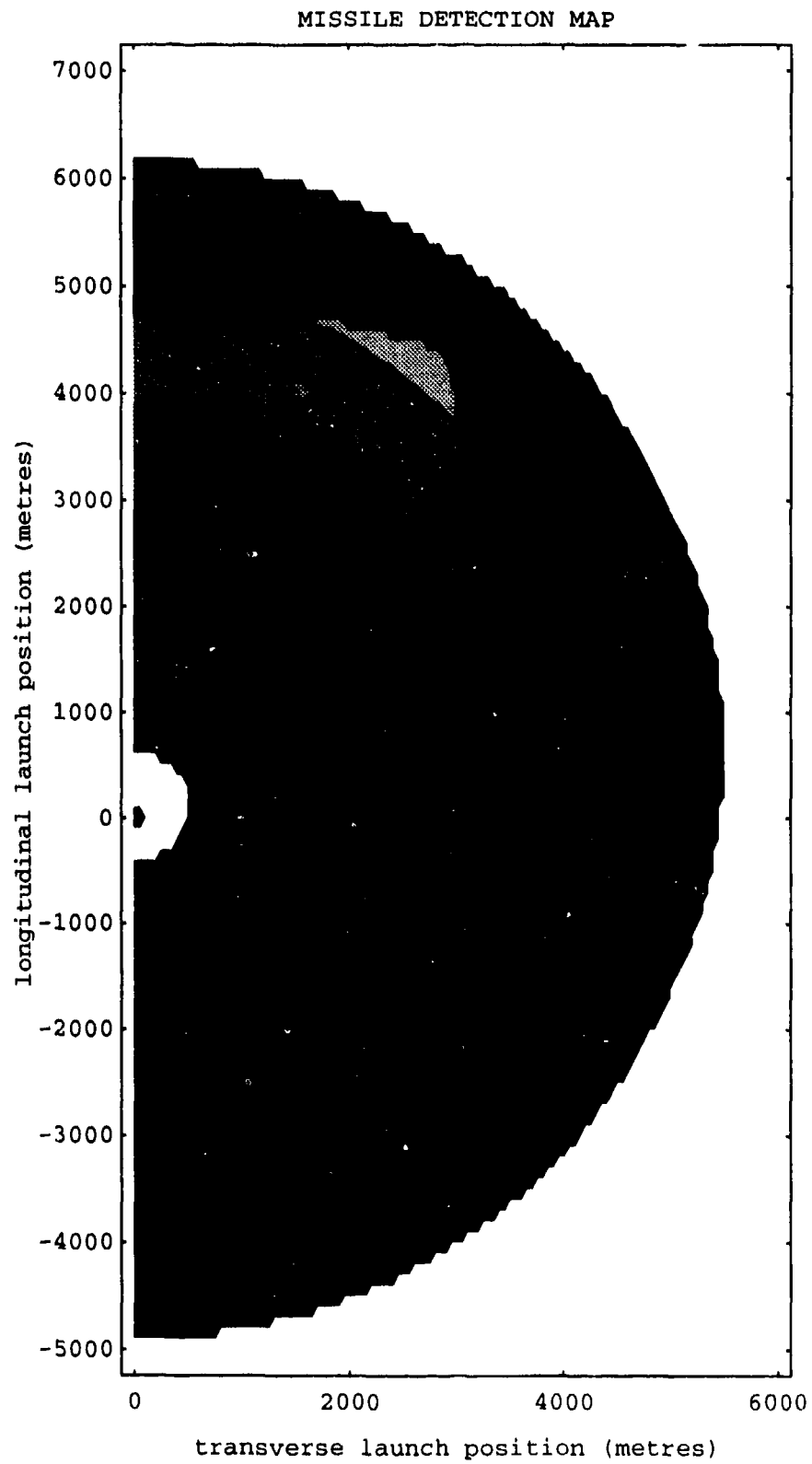
MISSILE DETECTION MAP

Figure 3: (c) Time interval for differential displacement to develop = 16 frames.

Figure 4

(next three pages)

List of common parameter values.

Number of pixels in the x direction = 512
Number of pixels in the y direction = 512
Pixel period in the x direction = 50.0 μm
Pixel period in the y direction = 50.0 μm
Field of view cone half angle = 80.0°
Frame rate = 25.0 s^{-1}
Detection threshold displacement = 2.00 pixels
Required consecutive missile detections = 4
Initial height of aircraft = 397.0 m
Upwards elevation = 8.0°
Aircraft ground speed = 173.0 km/h

Warning times (seconds) corresponding to intensity levels:
- 0 (no warning; black region)
- 0–2
- 2–4
- 4–6
- 6–8
- 8–10
- ∞ (no engagement; white region)

26

MISSILE DETECTION MAP
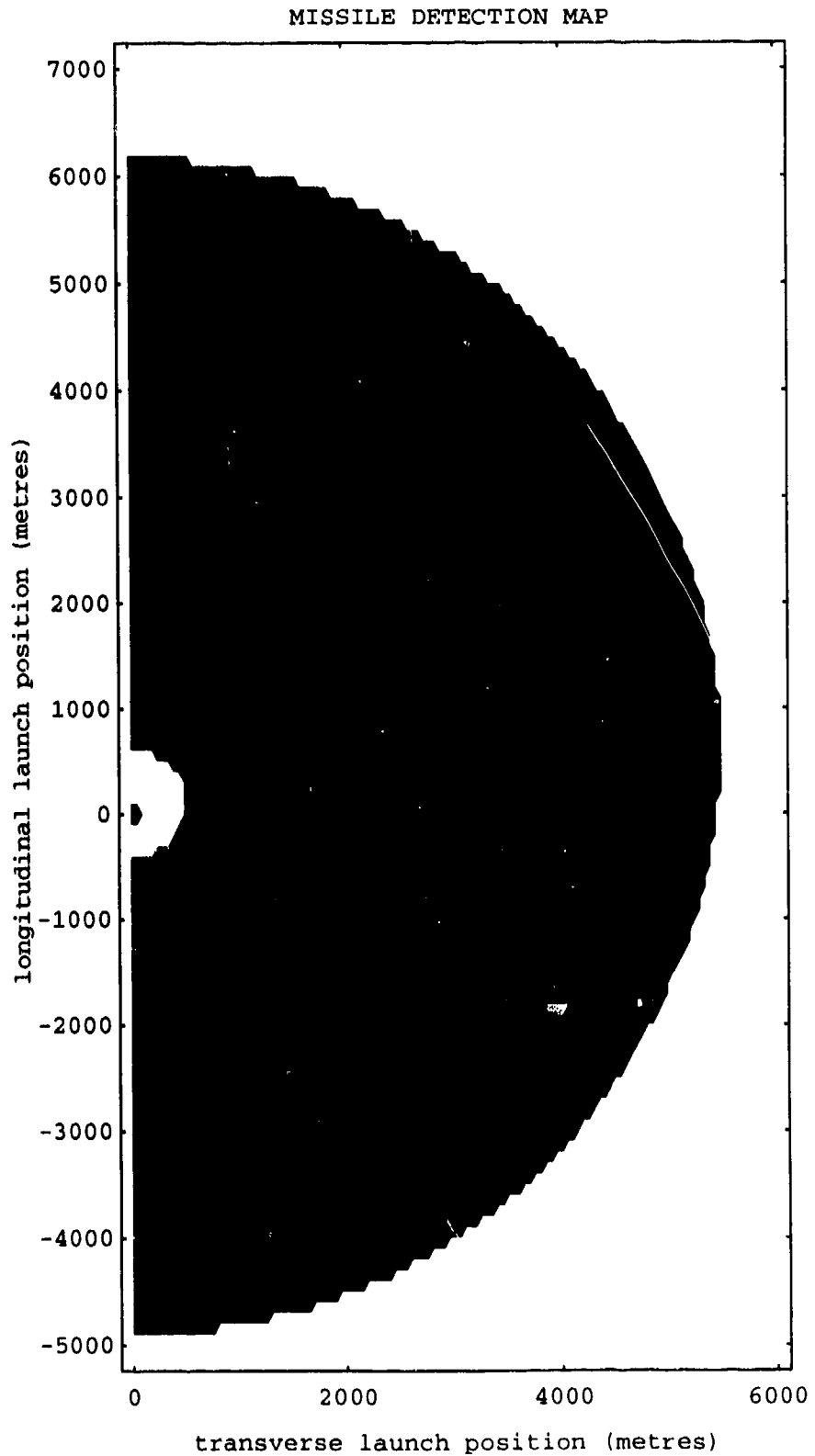
Figure 4: (a) Time interval for differential displacement to develop = 10 frames.

27

MISSILE DETECTION MAP
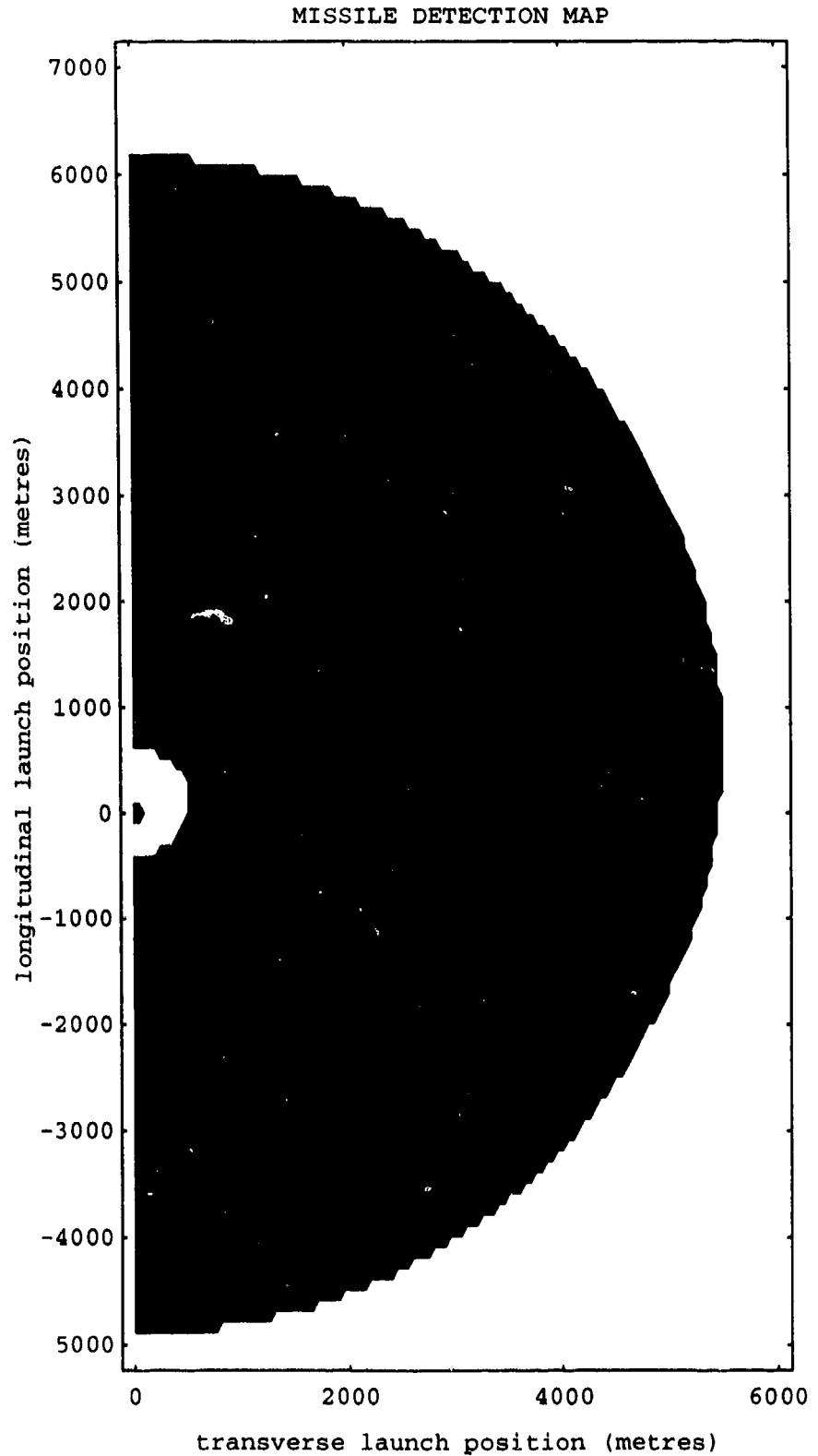
Figure 4: (b) Time interval for differential displacement to develop = 13 frames.
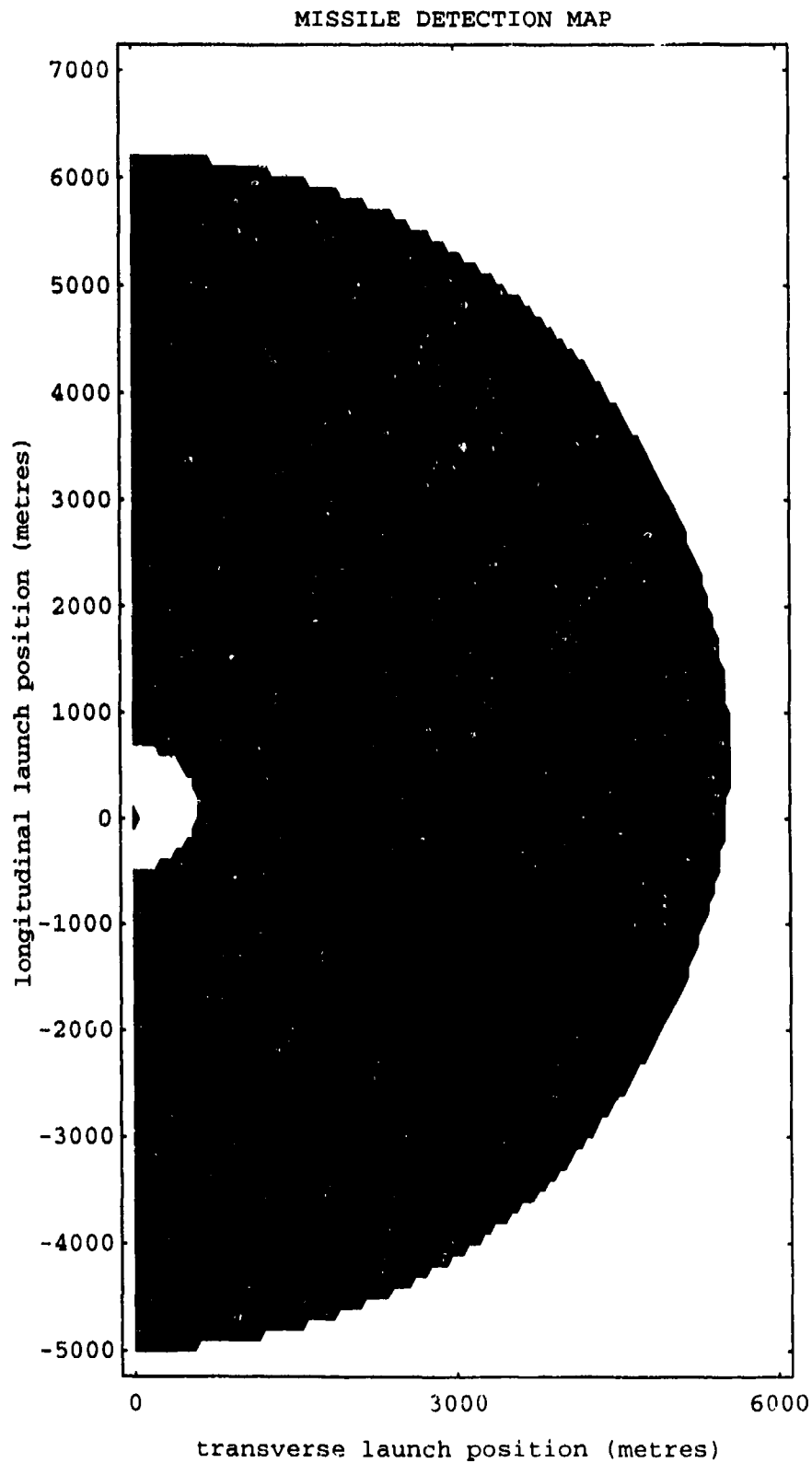
MISSILE DETECTION MAP

Figure 4: (c) Time interval for differential displacement to develop = 18 frames.

Figure 5

(next three pages)
List of common parameter values.

Number of pixels in the x direction = 512
Number of pixels in the y direction = 512
Pixel period in the x direction = 50.0 μm
Pixel period in the y direction = 50.0 μm
Field of view cone half angle = 80.0°
Frame rate = 25.0 s^{-1}
Detection threshold displacement = 2.00 pixels
Required consecutive missile detections = 4
Initial height of aircraft = 277.0 m
Upwards elevation = 0.0°
Aircraft ground speed = 159.0 km/h

Warning times (seconds) corresponding to intensity levels:
- 0 (no warning; black region)
- 0--1
- 1–2
- 2–3
- 3–4
- ∞ (no engagement; white region)

MISSILE DETECTION MAP
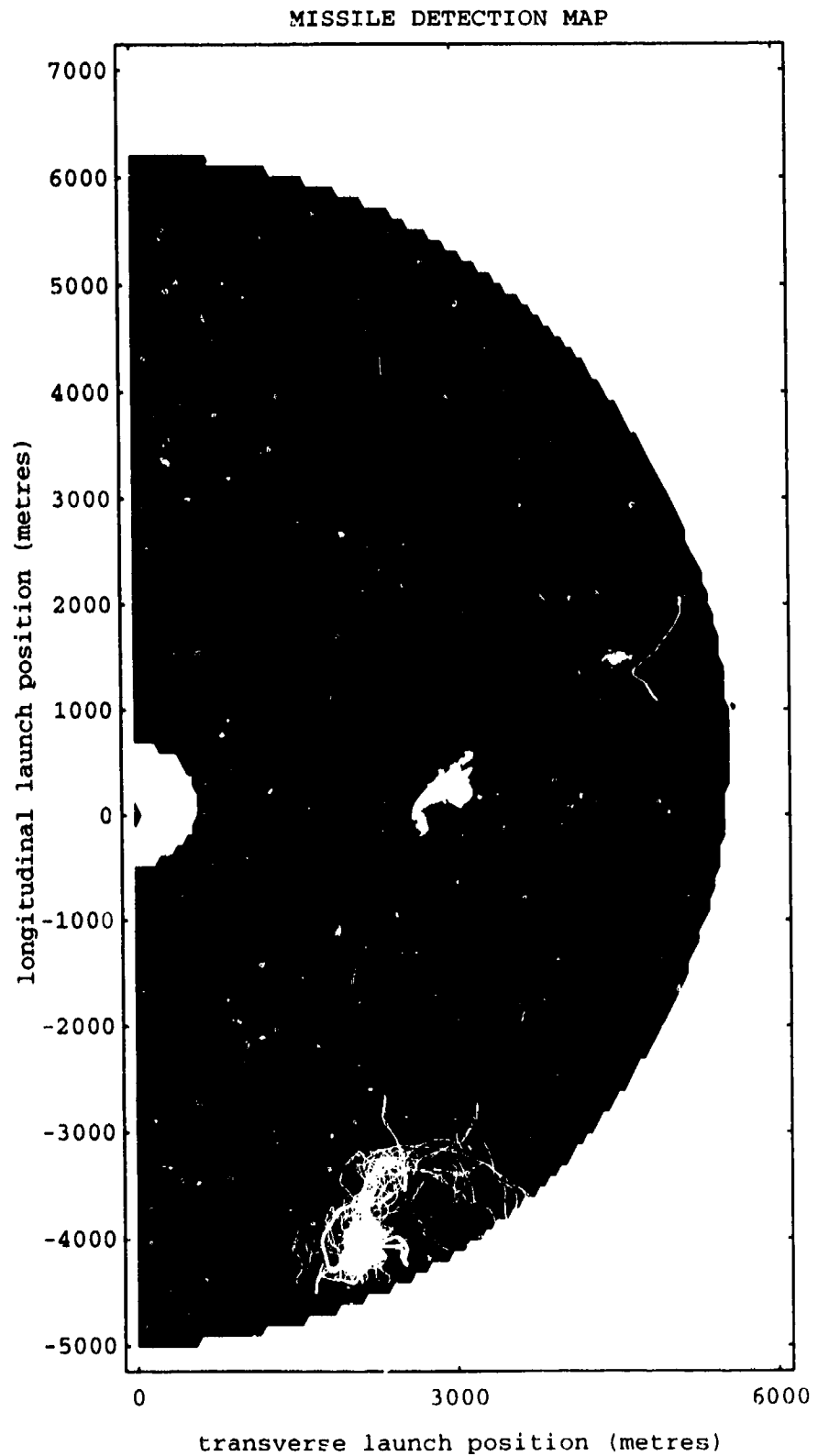
Figure 5: (a) Time interval for differential displacement to develop = 12 frames.

MISSILE DETECTION MAP
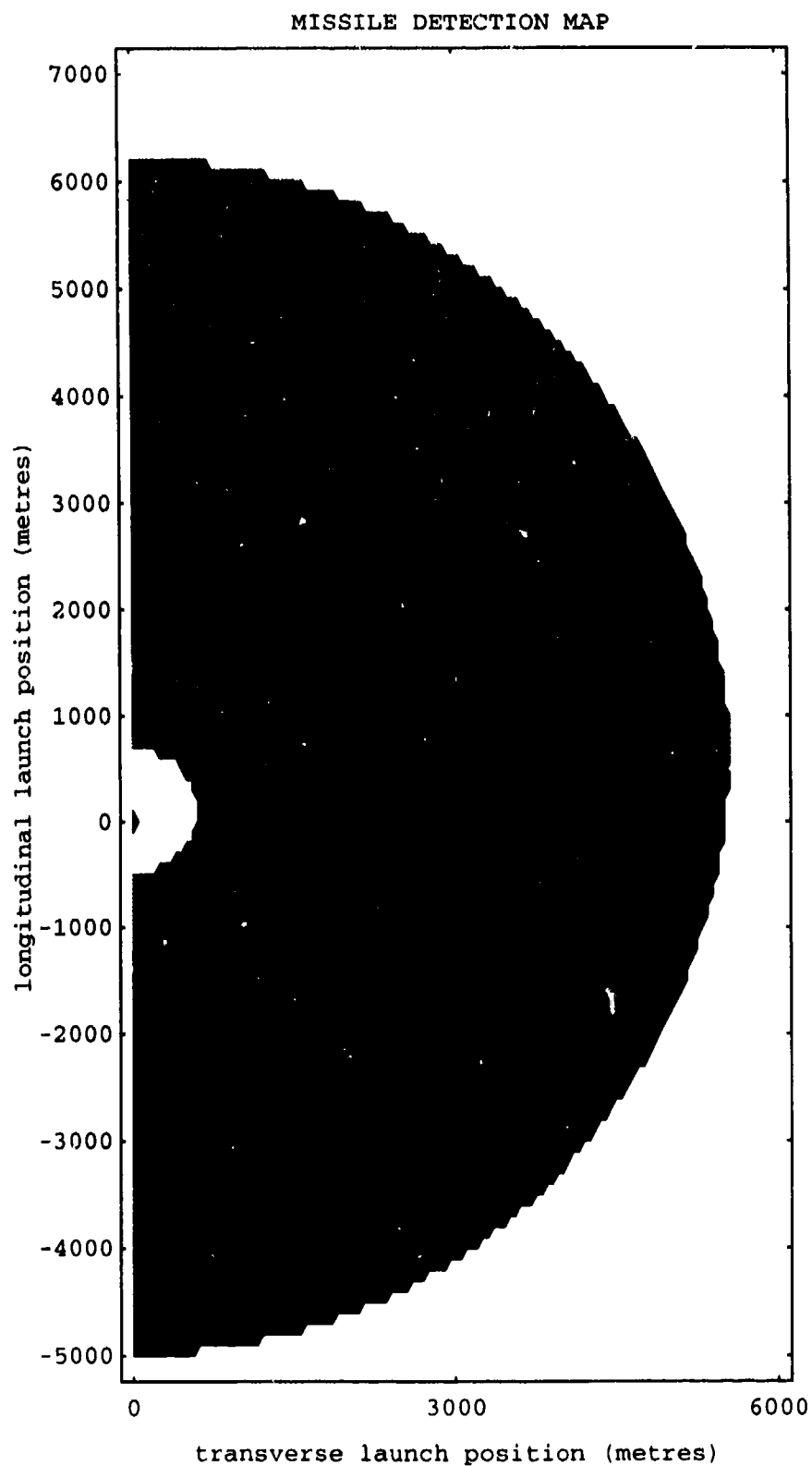
Figure 5: (b) Time interval for differential displacement to develop = 25 frames.

MISSILE DETECTION MAP

Figure 5: (c) Time interval for differential displacement to develop = 50 frames.

Figure 6

(next three pages)

List of common parameter values.

Number of pixels in the x direction = 512

Number of pixels in the y direction = 512

Pixel period in the x direction = 50.0 μm

Pixel period in the y direction = 50.0 μm

Field of view cone half angle = 90.0°

Frame rate = 25.0 s^{-1}

Detection threshold displacement = 2.00 pixels

Required consecutive missile detections = 4

Initial height of aircraft = 168.0 m

Upwards elevation = 0.0°

Aircraft ground speed = 580.0 km/h

Warning times (seconds) corresponding to intensity levels:
- 0 (no warning; black region)
- 0-3
- 3-6
- 6-9
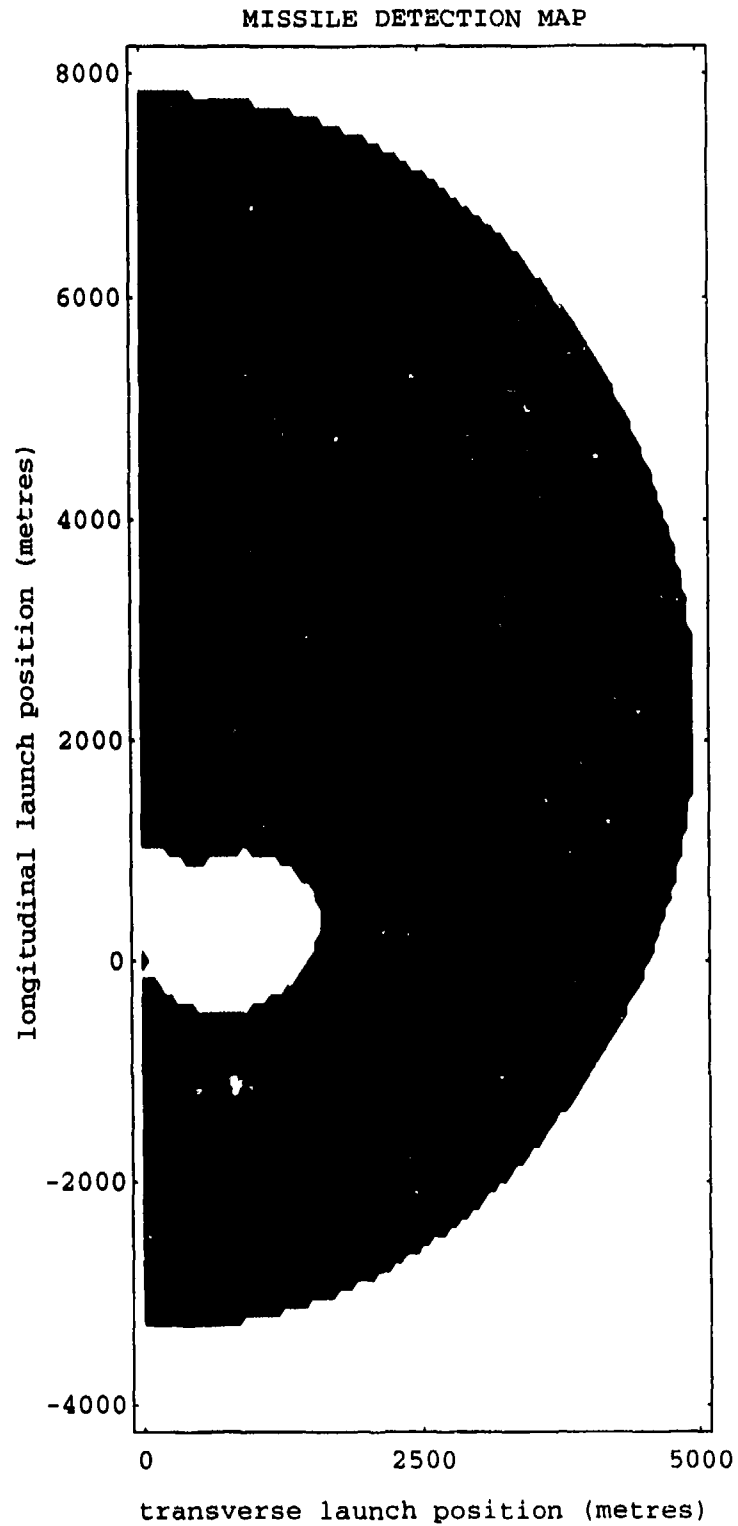- 9-12
- 12-15
- ∞ (no engagement; white region)

MISSILE DETECTION MAP

Figure 6: (a) Time interval for differential displacement to develop = 5 frames.

MISSILE DETECTION MAP
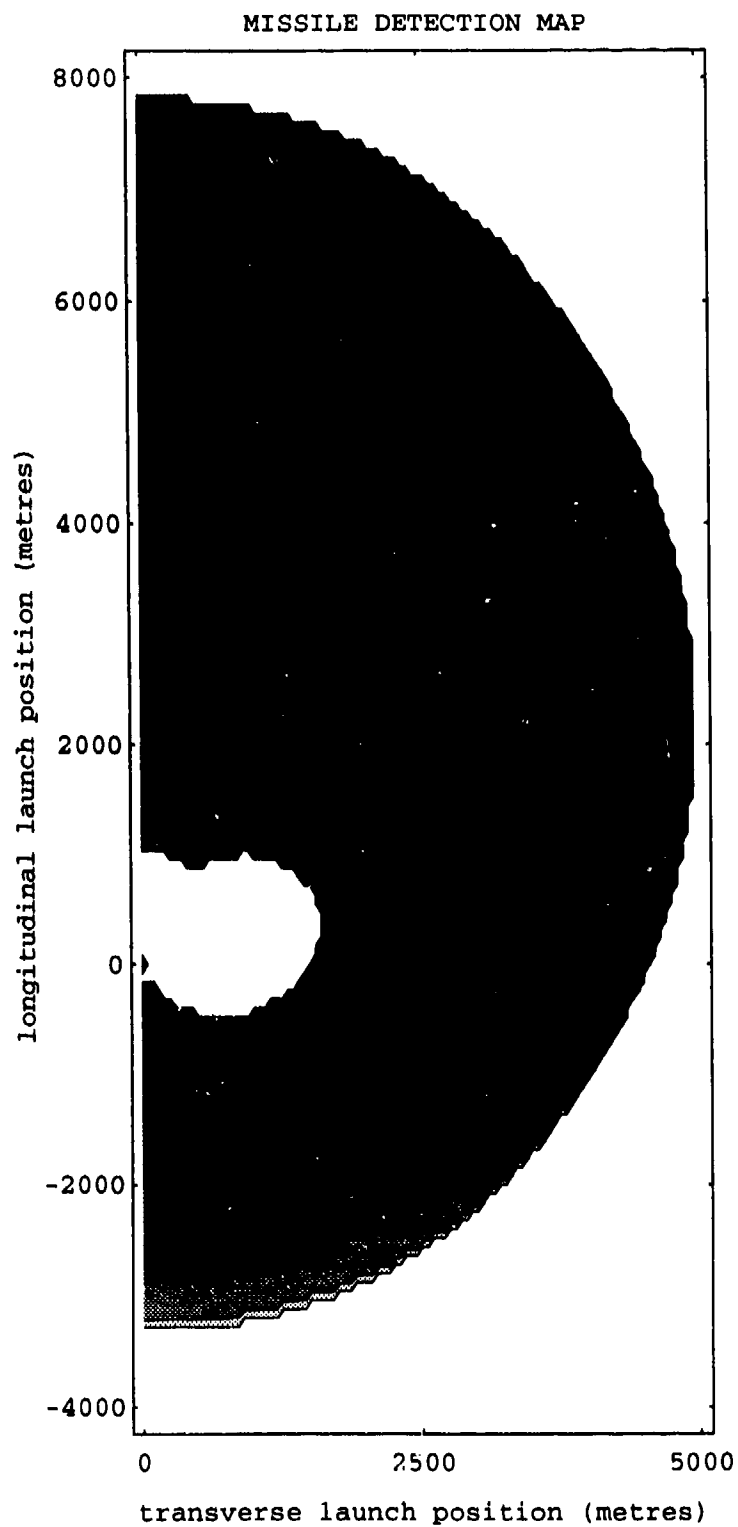
Figure 6: (b) Time interval for differential displacement to develop = 10 frames.
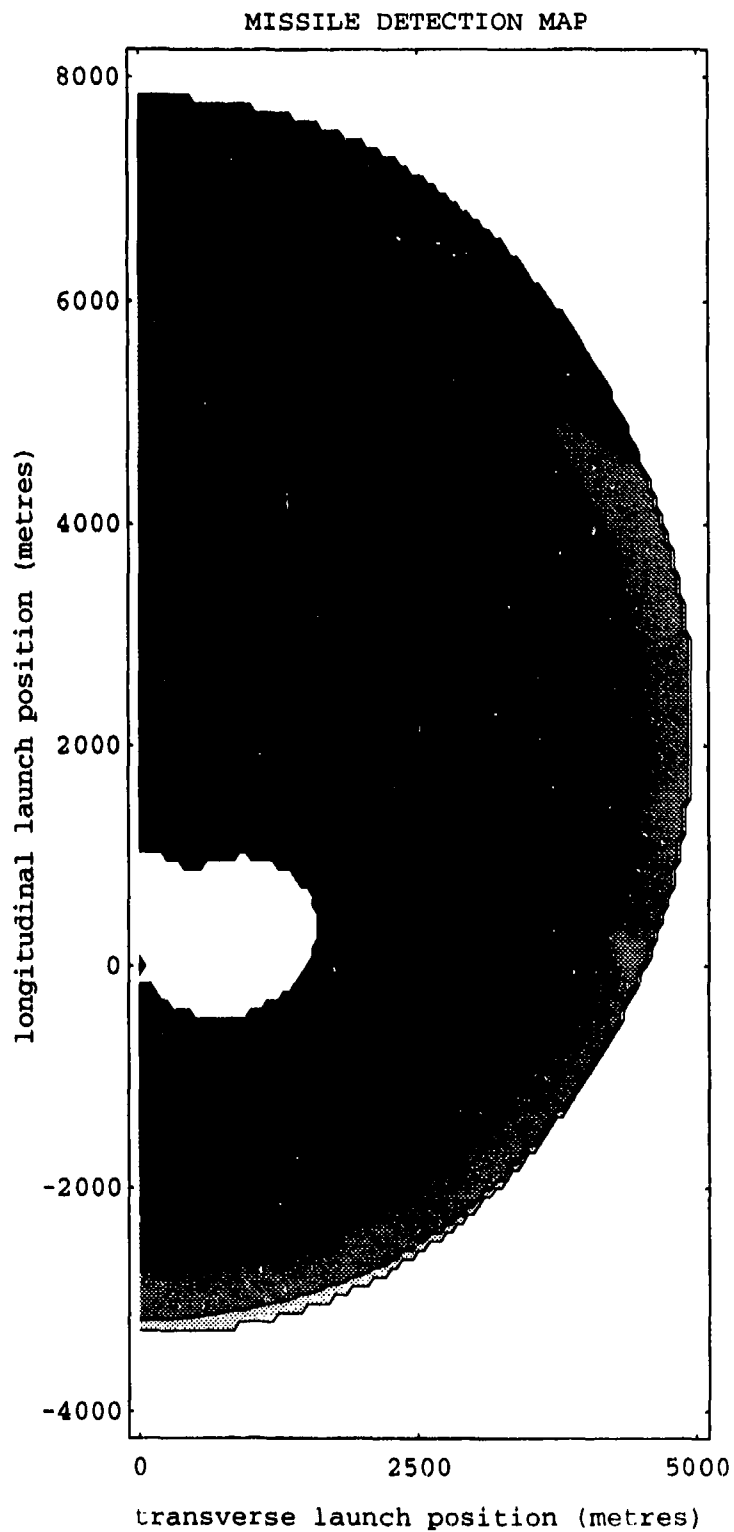
MISSILE DETECTION MAP

Figure 6: (c) Time interval for differential displacement to develop = 20 frames.

37

Figure 7
(next three pages)
List of common parameter values.

Number of pixels in the x direction = 512
Number of pixels in the y direction = 512
Pixel period in the x direction = 50.0 μm
Pixel period in the y direction = 50.0 μm
Field of view cone half angle = 80.0°
Frame rate = 25.0 s^{-1}
Detection threshold displacement = 2.00 pixels
Required consecutive missile detections = 4
Initial height of aircraft = 2307.0 m
Upwards elevation = 0.0°
Aircraft ground speed = 322.0 km/h

Warning times (seconds) corresponding to intensity levels:
- 0 (no warning; black region)
- 0-3
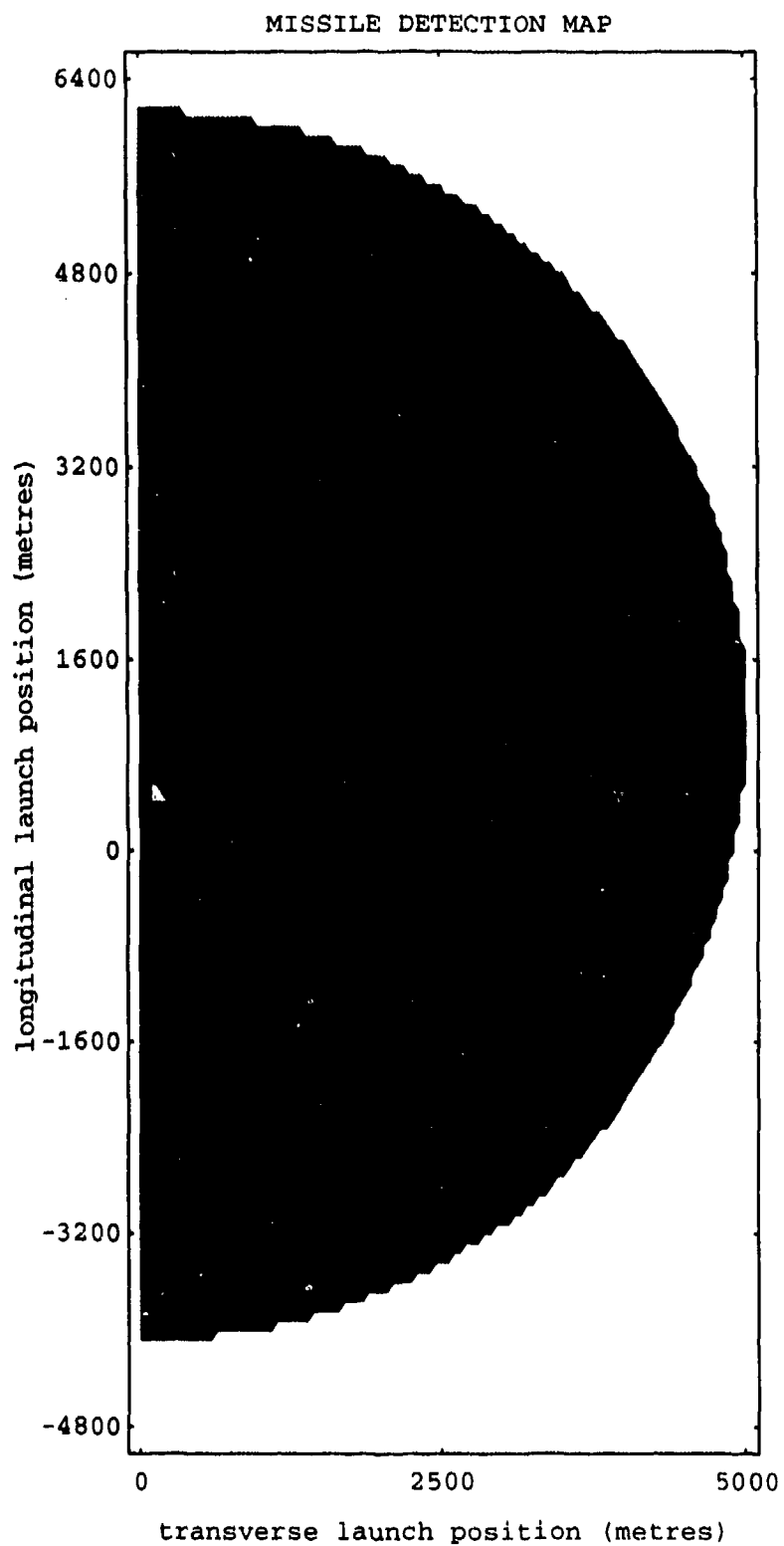- 3-6
- 6-9
- 9-12
- ∞ (no engagement; white region)

MISSILE DETECTION MAP

Figure 7: (a) Time interval for differential displacement to develop = 3 frames.

MISSILE DETECTION MAP
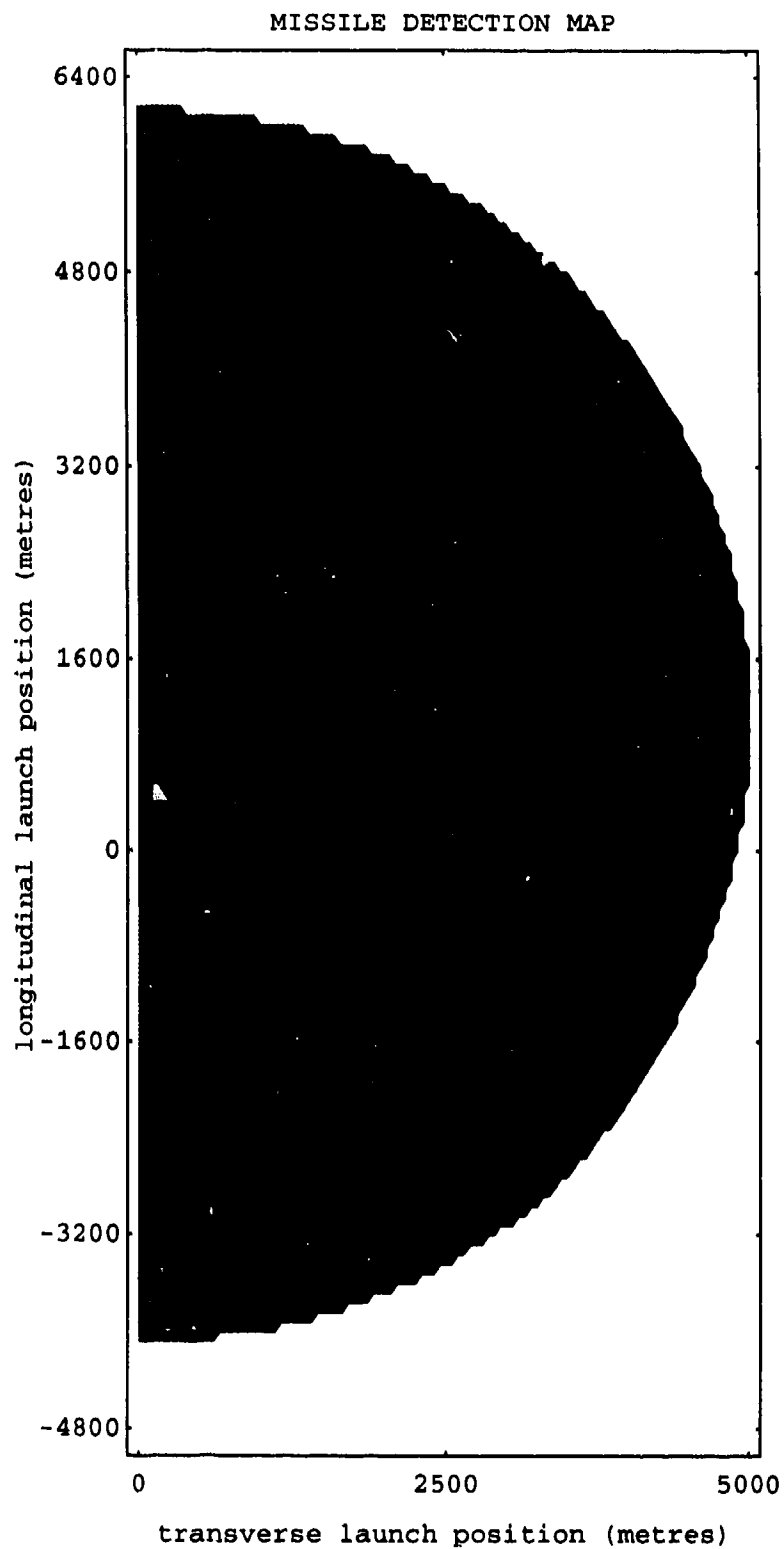
Figure 7: (b) Time interval for differential displacement to develop = 7 frames.
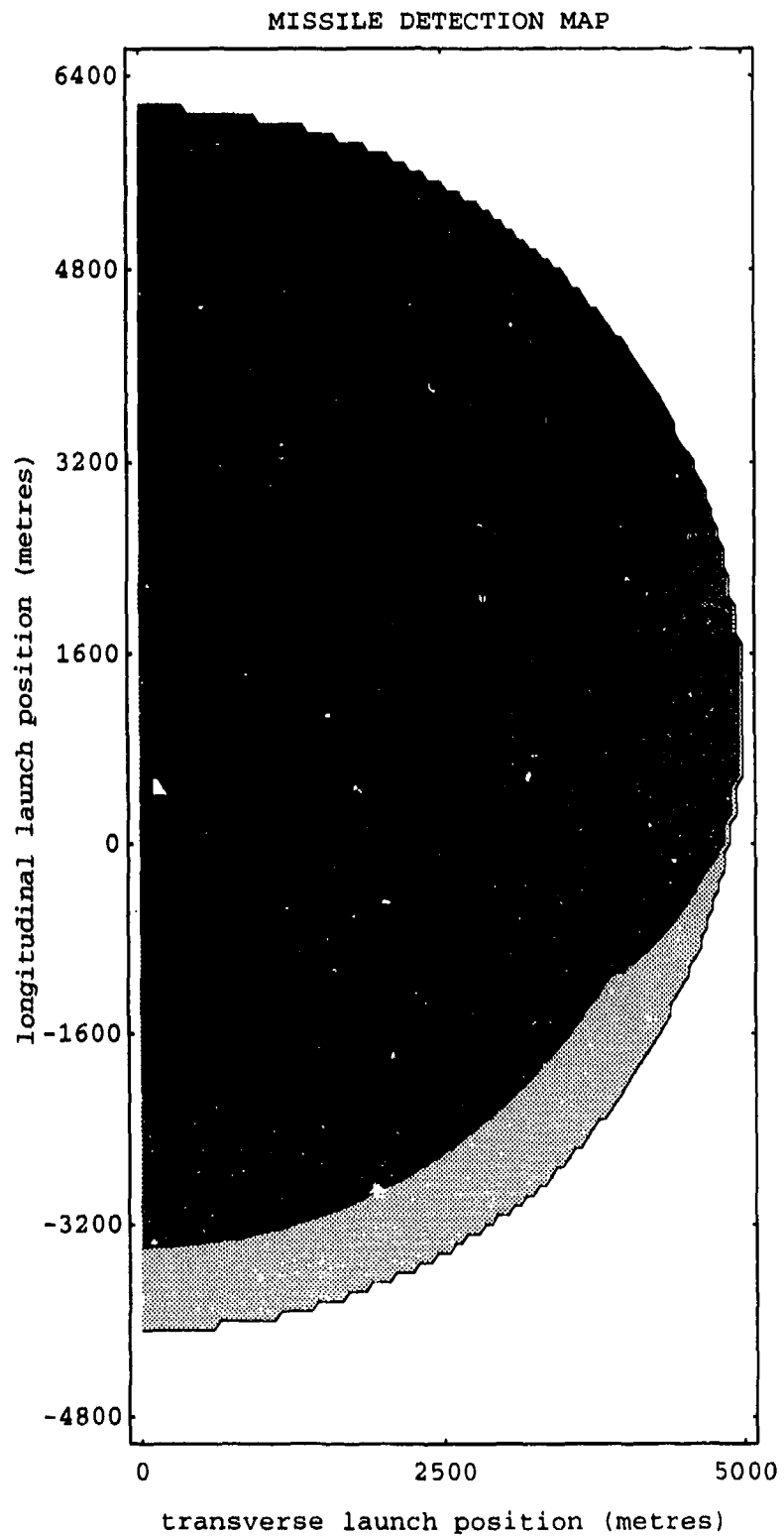
40

MISSILE DETECTION MAP

Figure 7: (c) Time interval for differential displacement to develop = 12 frames.

41

Figure 8

(next three pages)
List of common parameter values.

Number of pixels in the x direction = 512
Number of pixels in the y direction = 512
Pixel period in the x direction = 50.0 μm
Pixel period in the y direction = 50.0 μm
Field of view cone half angle = 80.0°
Frame rate = 25.0 s^{-1}
Detection threshold displacement = 2.00 pixels
Required consecutive missile detections = 4
Initial height of aircraft = 824.0 m
Upwards elevation = 0.0°
Aircraft ground speed = 119.0 km/h

Warning times (seconds) corresponding to intensity levels:
- 0 (no warning; black region)
- 0–2
- 2–4
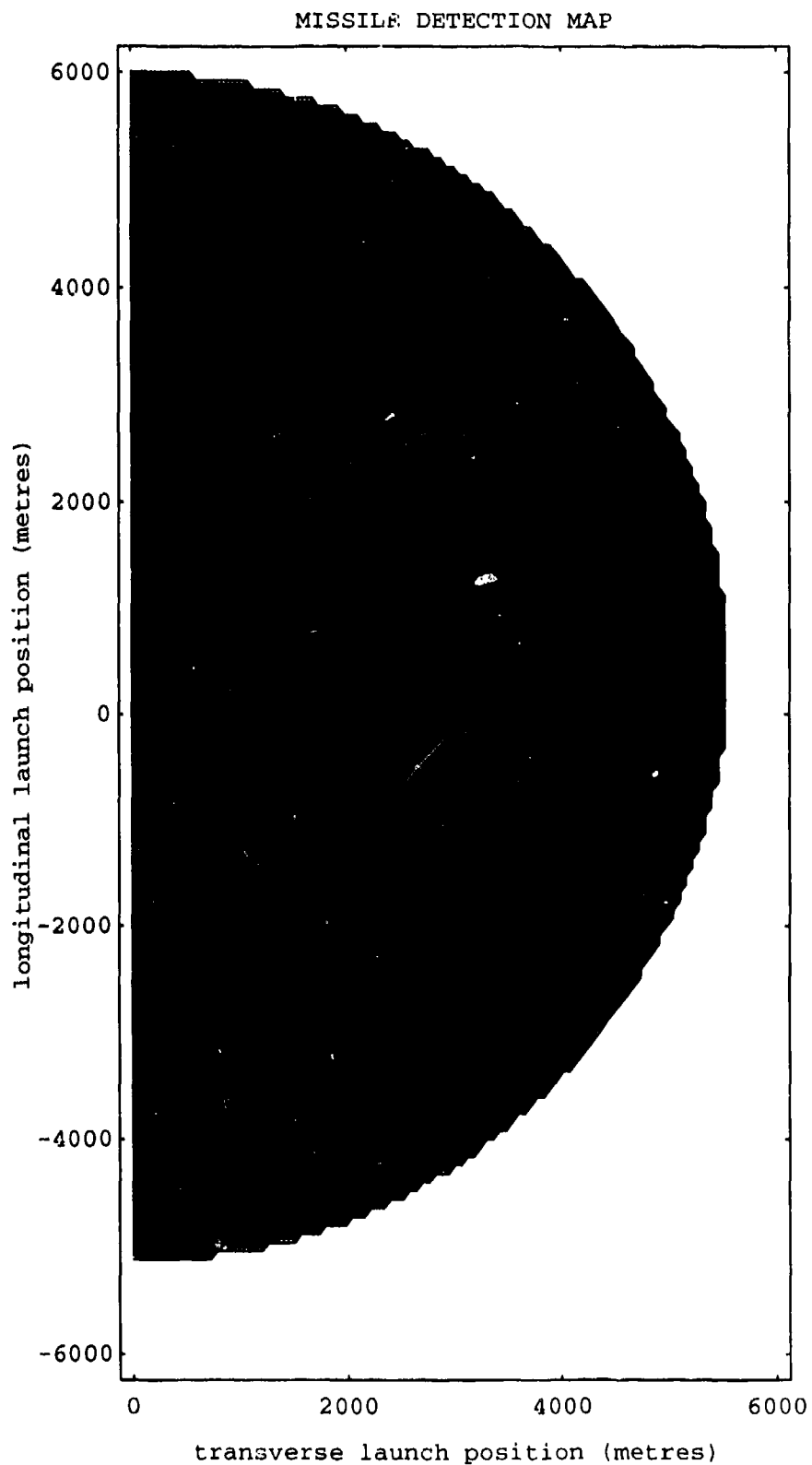- 4–6
- ∞ (no engagement; white region)

MISSILE DETECTION MAP

Figure 8: (a) Time interval for differential displacement to develop = 5 frames.

43

MISSILE DETECTION MAP
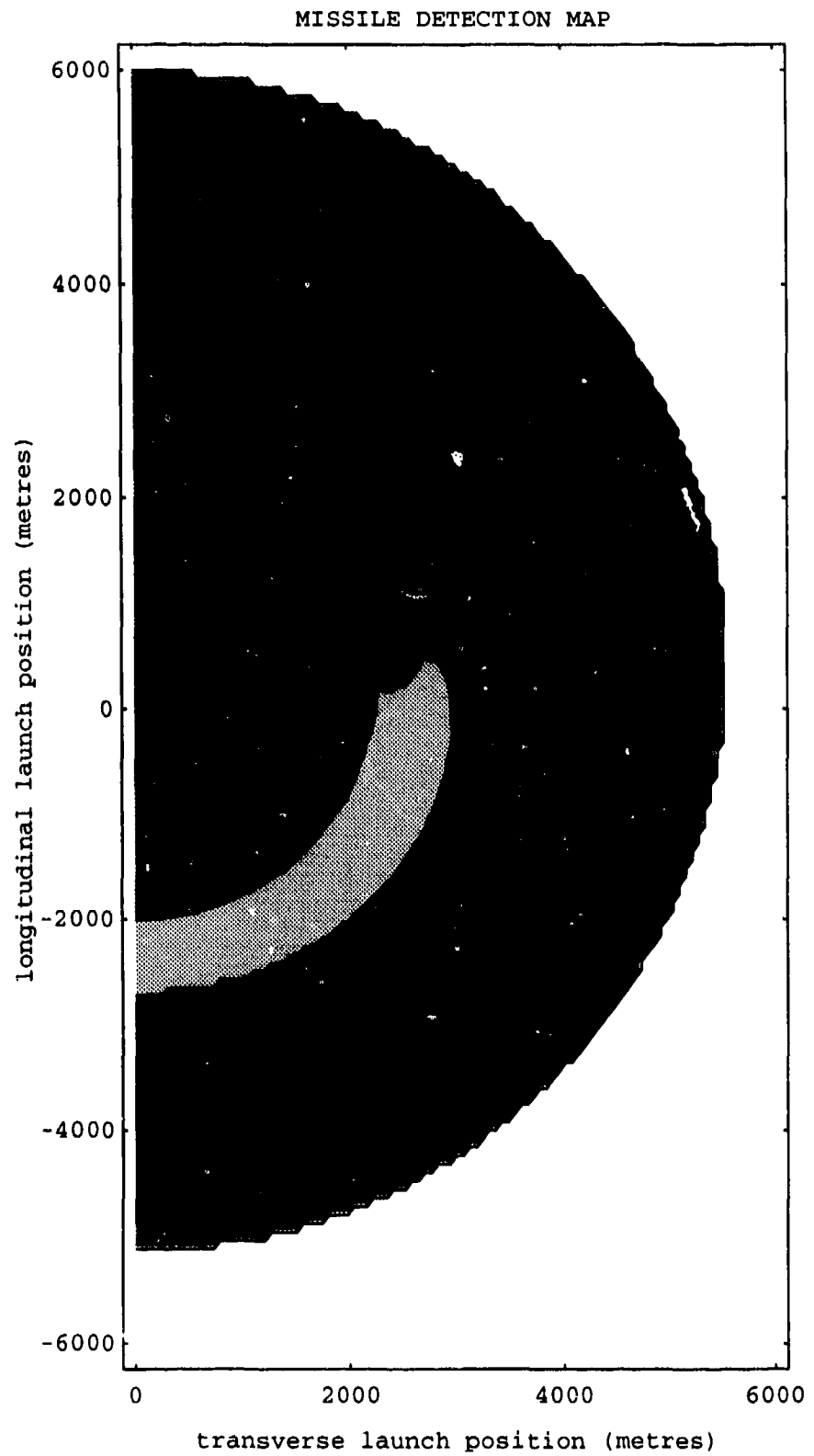
Figure 8: (b) Time interval for differential displacement to develop = 15 frames.

44

MISSILE DETECTION MAP

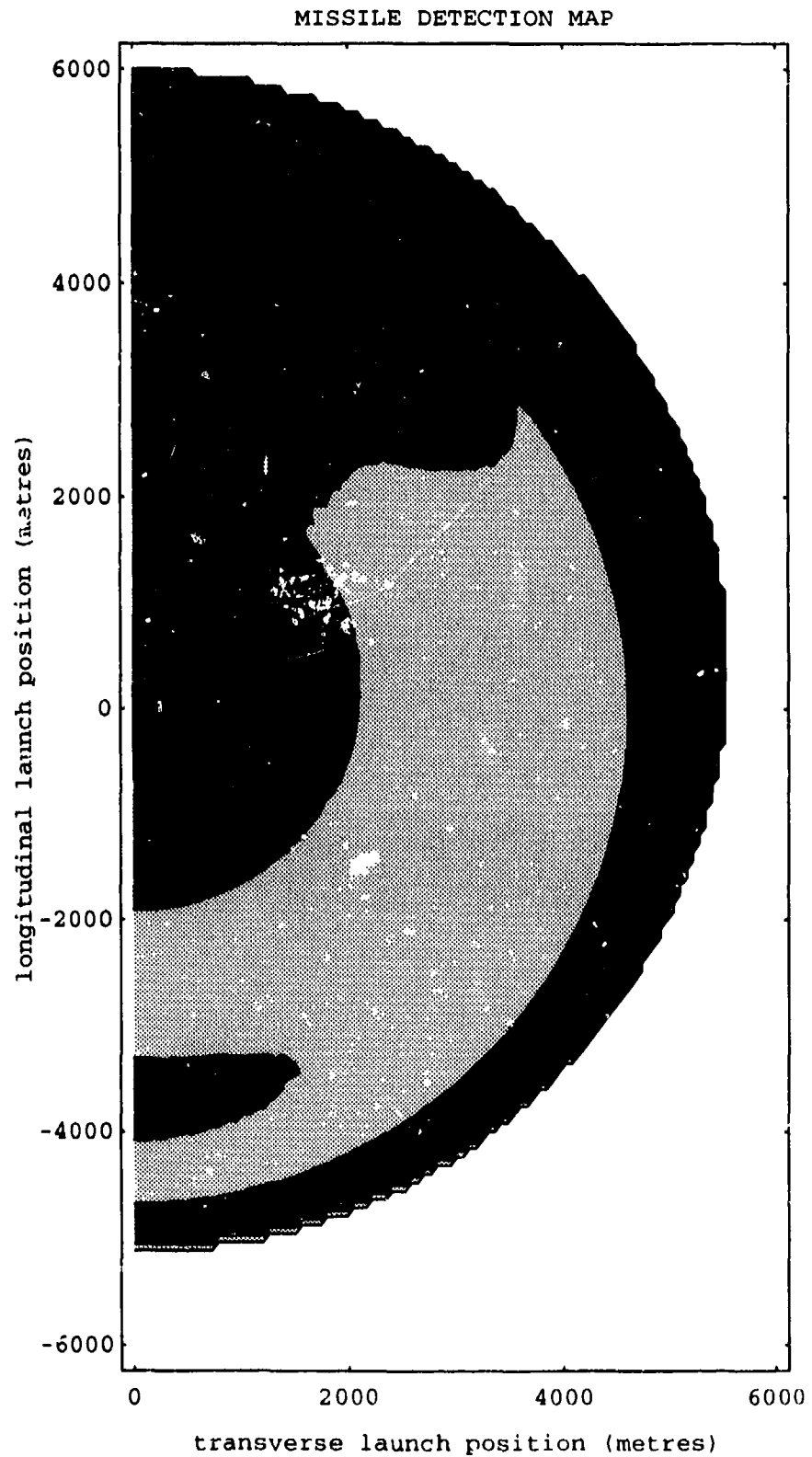*Figure 8: (c) Time interval for differential displacement to develop = 25 frames.*

45

THIS PAGE IS INTENTIONALLY BLANK

Missile Detection by Observation of Differential Motion in an Image Sequence [U]

Distribution

Copy Number

DEPARTMENT OF DEFENCE

HQ ADF

DSA (Air)   1

Defence Science and Technology Organisation

Chief Defence Scientist }

DSTO Central Office Executive }   2

Counsellor, Defence Science, London   Doc Cntl Sht

Counsellor, Defence Science, Washington   Doc Cntl Sht

Scientific Adviser, POLCOM }

Senior Defence Scientific Adviser }   3

Assistant Secretary, Scientific Analysis   4

Navy Office

Navy Scientific Adviser   5

Air Office

Air Force Scientific Adviser   6

Army Office

Scientific Adviser, Army   7

Aeronautical and Maritime Research Laboratory

Director, Aeronautical and Maritime Research Laboratory   8

Electronics and Surveillance Research Laboratory

Chief, Land, Space and Optoelectronics Division   9

Research Leader, Space and Surveillance Systems   10

Head, Image Processing Discipline   11

Author   12 to 13

Mr R. Johnson, WSD   14

Dr S. Kelly, EWD   15

<div align="center">

Department of Defence

DOCUMENT CONTROL DATA SHEET

</div>

1. Page Classification UNCLASSIFIED			
2. Privacy Marking/Caveat (of document) N/A			

3a. AR Number AR-009-403	3b. Laboratory Number DSTO-RR-0018	3c. Type of Report DSTO RESEARCH REPORT	4. Task Number ADA 94/132
5. Document Date October 1995	**6. Cost Code** 838298	**7. Security Classification**	**8. No of Pages** 52

10. Title
Missile detection by observation of differential motion in an image sequence

7. Security Classification

* R   U   U

Document   Title   Abstract

S (Secret) C (Confi) R (Rest) U (Unclas

* For UNCLASSIFIED docs with a secondary distribution LIMITATION, use (L) in document box.

9. No of Refs 8

11. Author(s)

Robert S. Caprari

12. Downgrading/Delimiting Instructions
Classification to be reviewed by 31/10/97.

13a. Corporate Author and Address

Electronics & Surveillance Research Laboratory
PO Box 1500, Salisbury SA 5108

13b. Task Sponsor
DGFD(A)

14. Officer/Position responsible for

Security: ....SOESRL..

Downgrading: ....SOESRL..

Approval for Release: .....CLSOD.

15. Secondary Release Statement of this Document
Access additional to the initial distribution list is limited to the defence communities of Aus., UK, USA, Can. and NZ.
Other access must be referred to the Director, ESRL.

16a. Deliberate Announcement
No limitation.

16b. Casual Announcement (for citation in other documents)
No limitation.

17. DEFTEST Descriptors
Missile detection, Aircraft defence, Differential motion, Temporal image processing, Warning time simulations, Kinematics.

18. DISCAT Subject Codes

19. Abstract
This report investigates a technique of passive airborne missile detection by analysing a temporal sequence of images of the ground in the region of the aircraft. Essentially, the technique identifies as potential missiles, objects that move in a different manner to the terrestrial background, as observed in the aircraft reference frame. A kinematical analysis is undertaken to quantify this "differential motion". Brief consideration is given to the observation of this differential motion by image processing techniques. The potential of the technique to localise the missile in space is addressed. The formal kinematics are applied to numerical simulations of guided missile trajectories to quantify the differential motion that occurs, and determine the "warning time" between missile detection and collision. Several operational scenarios are investigated. Simulation results are presented, discussed and appraised, and conclusions drawn about the effectiveness of this technique.